

The Role of Dissolved Hydrogen on the Corrosion/Dissolution of Spent Nuclear Fuel

NWMO TR-2008-19

November 2008

David W. Shoesmith

The University of Western Ontario

nwmo

NUCLEAR WASTE
MANAGEMENT
ORGANIZATION

SOCIÉTÉ DE GESTION
DES DÉCHETS
NUCLÉAIRES



Nuclear Waste Management Organization
22 St. Clair Avenue East, 6th Floor
Toronto, Ontario
M4T 2S3
Canada

Tel: 416-934-9814
Web: www.nwmo.ca

The Role of Dissolved Hydrogen on the Corrosion/Dissolution of Spent Nuclear Fuel

NWMO TR-2008-19

November 2008

David W. Shoesmith
The University of Western Ontario

Disclaimer:

This report does not necessarily reflect the views or position of the Nuclear Waste Management Organization, its directors, officers, employees and agents (the "NWMO") and unless otherwise specifically stated, is made available to the public by the NWMO for information only. The contents of this report reflect the views of the author(s) who are solely responsible for the text and its conclusions as well as the accuracy of any data used in its creation. The NWMO does not make any warranty, express or implied, or assume any legal liability or responsibility for the accuracy, completeness, or usefulness of any information disclosed, or represent that the use of any information would not infringe privately owned rights. Any reference to a specific commercial product, process or service by trade name, trademark, manufacturer, or otherwise, does not constitute or imply its endorsement, recommendation, or preference by NWMO.

ABSTRACT

Title: The Role of Dissolved Hydrogen on the Corrosion/Dissolution of Spent Nuclear Fuel
Report No.: NWMO TR-2008-19
Author(s): David W. Shoesmith
Company: The University of Western Ontario
Date: November 2008

Abstract

The literature on nuclear fuel dissolution and radionuclide release studies in aqueous solutions containing dissolved hydrogen has been reviewed. These studies include investigations with spent PWR and MOX fuels, fuel specimens doped with alpha emitters to mimic "aged" fuels, SIMFUELS fabricated to simulate spent fuel properties, and unirradiated uranium dioxide pellets and powders. In all these studies, dissolved hydrogen was shown to suppress fuel corrosion and in spent fuel studies to suppress radionuclide release.

A number of mechanisms have been either demonstrated or proposed to explain these effects, all of which involve the activation of hydrogen to produce the strongly reducing H^\bullet radical, which scavenges radiolytic oxidants and suppresses fuel oxidation and dissolution (i.e., corrosion). Both gamma and alpha radiation have been shown to produce H^\bullet surface species. With gamma radiation this could involve the absorption of gamma energy by the solid leading to water decomposition to OH^\bullet and H^\bullet radicals, with the OH^\bullet radical subsequently reacting with hydrogen to yield an additional H^\bullet . This latter radical then suppresses fuel oxidation and scavenges radiolytic oxidants. With alpha radiation, the need to neutralize oxygen vacancies generated by recoil events can initiate the same process by decomposing water. In the absence of radiation fields activation can occur on the surface of noble metal (epsilon) particles. Since these particles are galvanically-coupled to the fuel matrix they act as anodes for hydrogen oxidation (which proceeds through surface H^\bullet species) and forces the UO_2 to adopt a low potential. Also, there is some evidence to suggest that H_2 can be activated on the UO_2 surface in the presence of hydrogen peroxide, but the process appears to be inefficient.

Depending on the radiation fields present and the number density of epsilon particles, complete suppression of fuel corrosion appears possible even for hydrogen pressures as low as 0.1 to 1 bar. Since the corrosion of steel liners within failed waste containers could produce hydrogen pressures up to 50 bar, fuel corrosion could be completely suppressed under the long-term conditions expected in sealed repositories.

TABLE OF CONTENTS

	<u>Page</u>
ABSTRACT	v
1. INTRODUCTION	1
2. THE DEPENDENCE OF THE FUEL CORROSION/DISSOLUTION RATE ON REDOX CONDITIONS.....	2
3. INFLUENCES OF HYDROGEN ON FUEL CORROSION.....	6
3.1 Spent Fuels	6
3.2 Alpha-doped UO₂ Specimens.....	9
3.3 The Role of Gamma Radiation in the Activation of H₂	12
3.4 The Role of Alpha Radiolysis in the Activation of H₂	15
3.5 The Role of Noble Metal (Epsilon [ε]) Particles in the Control of Surface Redox Conditions	16
3.6 The Role of the UO₂ Surface in the Control of Surface Redox Conditions..	23
4. SUMMARY AND CONCLUSIONS	26
5. ACKNOWLEDGEMENTS	27
REFERENCES	27

LIST OF TABLES

	<u>Page</u>
Table 1: Exchange current densities for the proton reduction reaction for the four predominant epsilon particle constituents	16

LIST OF FIGURES

	<u>Page</u>
Figure 1: Alpha, beta, and gamma radiation dose rates calculated as a function of time for a layer of water in contact with a CANDU fuel bundle with a burnup of 220 MWh/kgU.....	2
Figure 2: The composition of a UO ₂ surface as a function of potential. The arrow A indicates the corrosion potential range predicted by a mixed potential model to describe fuel corrosion due to the alpha radiolysis of water inside a failed waste container (Shoesmith et al. 2003). The upper limit of this range represents the expected E _{CORR} if the container fails soon after emplacement in the repository, and the lower limit represents the E _{CORR} predicted if the container fails after 10 ⁶ years.	3
Figure 3: Illustration showing the key chemical and electrochemical reactions anticipated inside a groundwater flooded waste container.....	4
Figure 4: Illustration showing the two corrosion fronts existing within a failed, groundwater-flooded waste container, one on the fuel surface established by reaction with radiolytic oxidants and a second one on the steel surface established by reaction with water. The zone marked E _h indicates the redox condition expected due to the alpha radiolysis of water. The E _{CORR} zones indicate the range of corrosion potentials measured on fuel and steel electrodes.	5
Figure 5: Used fuel dissolution rates as a function of pH for oxidizing and reducing conditions. Oxidizing conditions: solution purged with 20% O ₂ /0.03% CO ₂ / 80% Ar; Reducing conditions, solution bubbled with H ₂ containing 0.03% CO ₂ over a Pt foil (Rollin et al. 2001). The two horizontal lines are extrapolations of electrochemically measured corrosion rates to -0.35V and -0.45V (Shoesmith 2007).....	8
Figure 6: Corrosion rates measured for alpha-doped UO ₂ , non-doped UO ₂ (0.01 MBq/g) and spent fuel specimens as a function of alpha activity (Poinssot et al. 2005). The sources of the individual data points are given in the reference. The dashed lines are arbitrary and drawn to emphasize the approximate alpha-strength below which no influence of alpha radiation is observed (1 MBq/g).....	10
Figure 7: Measured H ₂ , O ₂ and total U concentrations, as a function of time, in a pressure vessel leaching experiment of a 10% ²³³ U-doped UO ₂ in 10 ⁻² mol/L NaCl (0 to 114 days) and 10 ⁻² mol/L NaCl + 2 x 10 ⁻² mol/L HCO ₃ ⁻ (114 days onwards) as the H ₂ overpressure was periodically changed. The red line shows the calculated radiolytic O ₂ concentrations (Carbol et al. 2005).	11

Figure 8: Time dependence of the corrosion potential (E_{CORR}) of a UO_2 electrode in gamma-irradiated 0.1 mol/L NaCl (pH~9.5) at room temperature in the presence of either 5MPa of H_2 or Ar. The results of four or five replicate tests are shown for each set of conditions. The range of E_{CORR} values recorded in unirradiated solutions for both gases is shown as the vertical bar (King and Shoesmith 2004).....	13
Figure 9: Effect of changing from H_2 (heavy line) to Ar (light line) overpressure on the E_{CORR} of UO_2 in γ -irradiated 0.1 mol·dm ⁻³ NaCl solution (pH 9.5) at room temperature (King et al. 1999).....	14
Figure 10: SIMS images showing the elements ^{96, 98} Mo, ^{102, 104} Ru, and ^{106, 108} Pd detected in three SIMFUEL specimens (SF) with various degrees of simulated burn-up (expressed as an atomic %). No map for Rh is shown due to its low concentration. Each individual area is 50 μ m x 50 μ m.	17
Figure 11: E_{CORR} measurements on a SIMFUEL electrode (SF1.5, with an extent of simulated burn-up of 1.5 at %) in a 0.1 mol/L KCl solution (pH = 9.5) purged with various gases at 60°C. The electrode was electrochemically-cleaned prior to the start of each experiment. The dashed line shows the potential threshold for corrosion (Figure 2) (Broczkowski et al. 2005).....	18
Figure 12: The influence of the increasing number and size of epsilon particles in SIMFUELS with different degrees of simulated burnup (expressed as an atomic %) on the corrosion potential (E_{CORR}) measured in H_2 -purged 0.1mol/L KCl solution (pH = 9.5) at 60°C. The horizontal line shows the potential threshold for corrosion (Figure 2) (Shoesmith 2007). ..	18
Figure 13: The influence of the increasing number and size of epsilon particles in SIMFUELS with different degrees of simulated burnup (expressed as an atomic %) on the degree of oxidation of the surface (determined by XPS) in H_2 -purged 0.1mol/L KCl (pH = 9.5) at 60°C. The horizontal line shows the potential threshold below for corrosion (Figure 2) (Shoesmith 2007).....	19
Figure 14: Illustration showing the galvanic coupling of epsilon particles to the fuel matrix in H_2 -containing solutions (Broczkowski et al. 2005).	20
Figure 15: The influence of H_2 solution overpressure on the E_{CORR} of a SIMFUEL electrode with 1.5% of simulated burn-up (SF1.5) measured in a 0.1 mol/L KCl solution (pH = 9.5) at 60°C. The system was initially purged with Ar only at atmospheric pressure, and then with a series of increasing 5% H_2 /Ar pressures (Broczkowski et al. 2005).....	20
Figure 16: E_{CORR} recorded on a SIMFUEL with 1.5% of simulated burn-up (SF1.5) in a 0.1 mol·L ⁻¹ KCl solution (pH 9.5) purged with Ar at 60°C. The arrows indicate the times when H_2O_2 was added in the individual experiments (Broczkowski 2008).....	21
Figure 17: E_{CORR} recorded on a SIMFUEL with 1.5% of simulated burn-up (SF1.5) in a 0.1 mol·L ⁻¹ KCl solution (pH 9.5) purged with 5% H_2 /95% Ar at 60°C. The arrows indicate the times when H_2O_2 was added in the individual experiments (Broczkowski 2008).....	22

- Figure 18: Surface composition measured (by XPS) on a SIMFUEL with 1.5% of simulated burn-up (SF1.5) after E_{CORR} measurements in 5% $H_2/95\%$ Ar-purged 0.1 mol/L KCl solution (pH = 9.5) at 60°C. The horizontal dotted lines refer to the fraction of U^{IV} (black), U^V (light grey), and U^{VI} (dark grey) measured after E_{CORR} experiments with no H_2O_2 added (Broczkowski 2008).23
- Figure 19: The influence of H_2 overpressure on the E_{CORR} of a SIMFUEL electrode with 3.0% simulated burn-up, but containing no epsilon particles, in a 0.1 mol/L KCl solution (pH = 9.5) at 60°C. The system was initially purged with Ar only at atmospheric pressure, and then with a series of increasing 5% H_2/Ar pressures (Broczkowski et al. 2005).....24
- Figure 20: E_{CORR} measured on a SIMFUEL with 3 at % simulated burn-up, but containing no epsilon particles in a 0.1 mol/L KCl solution (pH 9.5) purged with 5% $H_2/95\%$ Ar at 60°C. The arrows indicate the times when H_2O_2 was added in the individual experiments (Broczkowski 2008).25

1. INTRODUCTION

The selected approach for long-term management of used nuclear fuel in Canada is Adaptive Phased Management (NWMO 2005). This approach includes centralized containment and isolation of the used fuel in a deep geological repository in a suitable rock formation. The repository concept is based on multiple barriers, and provides reasonable assurance in the long-term containment and isolation of the fuel bundles. One of these barriers is the robust copper shell-steel lined container (McMurry et al. 2003; King and Kolar 2000; King and Kolar 1996; Maak 2003). However, it is judicious to assume containers will eventually fail, thereby, exposing the used fuel bundles to groundwater. Since the used fuel contains the residual radioactivity, its behaviour in contact with groundwater is important for long-term safety assurance.

The release of > 90% of radionuclides contained within the used nuclear fuel will be governed by the corrosion/dissolution of the fuel (UO_2) matrix. The rate of this process will be related to, but not necessarily directly proportional to, the solubility of uranium in the groundwater contacting the fuel. At repository depths, groundwaters are inevitably oxygen-free. Furthermore, any oxygen introduced during repository construction and operation prior to sealing will be rapidly consumed by mineral and biochemical reactions in the surrounding clays and by minor corrosion of the copper container (McMurry et al. 2003; King and Kolar 2000; King and Kolar 1996; Maak 2003).

If anoxic conditions were maintained in the repository, the solubility of the UO_2 waste form would be in the region of $\sim 10^{-9.5}$ mol/L, which is very low (Parks and Pohl 1988; Grenthe et al. 1992; Fuger 1993; Neck and Kim 2001; Rai et al. 2003; Yajima et al. 1995; Rai et al. 1990; Guillaumont et al. 2003). However, the radiolysis of water due to the radiation fields in the fuel will establish oxidizing conditions at the fuel surface. Under oxidizing conditions the solubility of uranium (as UO_2^{2+}) increases by many orders of magnitude (Grenthe et al. 1992). Thus, the rate of fuel dissolution (which is a corrosion reaction when oxidants are consumed to produce soluble UO_2^{2+}) will depend on the redox condition (Shoesmith 2000; Werme et al. 2004; Carbol et al. 2005) which will be established by the radiation fields associated with the fuel and how they decay with time. This is illustrated in Figure 1, which shows the evolution of radiation dose rates with time for a typical CANDU fuel bundle. This evolution in solution redox conditions makes the fuel corrosion process (and, hence, the radionuclide release process) very dependent on the time to failure of the waste container.

In this report the influence of redox conditions on fuel corrosion/dissolution inside a failed waste container will be discussed with a special emphasis on the effect of dissolved H_2 . Significant pressures of H_2 are expected to develop as the steel liner within the container corrodes, since its escape through the surrounding compacted clay and host rock will be very slow.

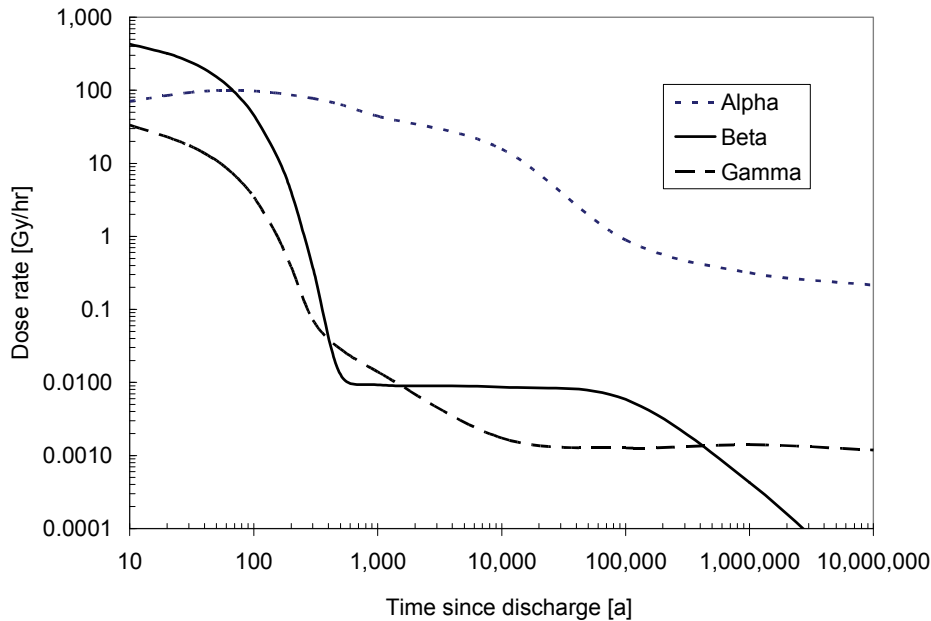


Figure 1: Alpha, beta, and gamma radiation dose rates calculated as a function of time for a layer of water in contact with a CANDU fuel bundle with a burnup of 220 MWh/kgU

2. THE DEPENDENCE OF THE FUEL CORROSION/DISSOLUTION RATE ON REDOX CONDITIONS

The dependence of fuel corrosion/dissolution rate on redox conditions is now well established based on electrochemical measurements (Shoesmith 2000; Shoesmith and Sunder 1991; Sunder et al. 2004; Shoesmith et al. 1989), measurements of corrosion rates (or rate constants) in the presence of oxidants (Ekeroth and Jonsson 2003; Hossain et al. 2006; Gimenez et al. 1996; de Pablo et al. 1996; de Pablo et al. 2001; Clarens et al. 2004; Corbel et al. 2006; de Pablo et al. 2004) and dissolution/corrosion rate measurements in the presence of radiation fields (Carbol et al. 2005; Corbel et al. 2006; Jegou et al. 2004; Mennecart et al. 2004; Stroes-Gascoyne and Betteridge 2005; Bailey et al. 1985; Sunder et al. 1992; Sunder et al. 1997; Wren et al. 2005).

Based on this data and additional electrochemical evidence (Santos et al. 2004; Shoesmith et al. 2004), the fuel behaviour can be specified as a function of redox conditions, Figure 2. In this plot, the potential axis is the corrosion potential (E_{CORR}), which specifies the response of the fuel surface to the redox condition (E_h) in the exposure environment. (Although not shown here, a plot of measured and predicted fuel corrosion rates as a function of potential has also been determined (Shoesmith 2000; Shoesmith et al. 2003)). The vertical dashed line in Figure 2 (at -0.4V [vs SCE]) indicates the threshold for the onset of fuel corrosion. Descriptions of the experimental procedures used to establish this threshold have been described elsewhere (Santos et al 2004; Shoesmith et al 2004; Shoesmith 2007). Above this potential there is the possibility of fuel corrosion at a rate controlled by the concentration of radiolytically-produced

oxidants. For potentials below this threshold, fuel dissolution, and hence the mobilization of radionuclides, can only occur by chemical dissolution of the UO_2 fuel (to yield soluble U^{IV}).

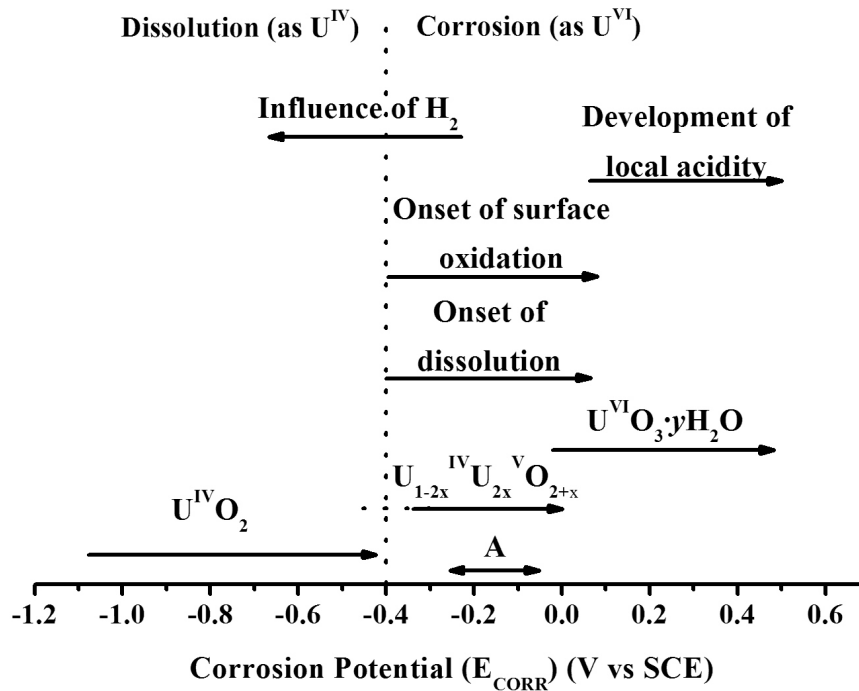


Figure 2: The composition of a UO_2 surface as a function of potential. The arrow A indicates the corrosion potential range predicted by a mixed potential model to describe fuel corrosion due to the alpha radiolysis of water inside a failed waste container (Shoesmith et al. 2003). The upper limit of this range represents the expected E_{CORR} if the container fails soon after emplacement in the repository, and the lower limit represents the E_{CORR} predicted if the container fails after 10^6 years.

While the above studies establish the corrosion nature of the fuel dissolution/radionuclide release process and its dependence on redox conditions in the presence of radiolytically decomposed water, other processes occurring within a failed container would influence the redox conditions at the fuel surface. The key reactions anticipated within a failed, groundwater-flooded container are illustrated in Figure 3.

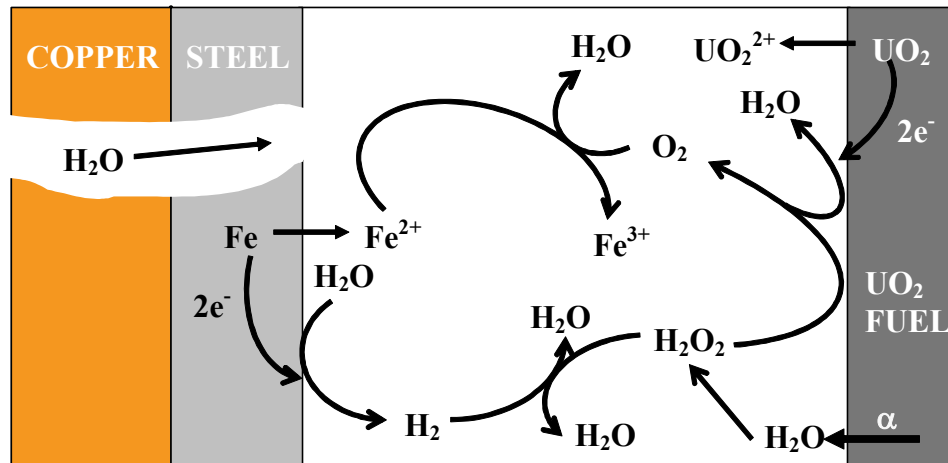


Figure 3: Illustration showing the key chemical and electrochemical reactions anticipated inside a groundwater flooded waste container.

Two corrosion fronts exist, one on the fuel surface driven by the radiolytic oxidants and a second one on the surface of the carbon steel liner sustained by reaction with water to produce Fe^{2+} and H_2 . In this illustration, H_2O_2 is taken to be the primary radiolytic oxidant driving fuel corrosion (Ekeroth et al. 2004; Ekeroth et al. 2006; Nielson and Jonsson 2006), although the production of O_2 via H_2O_2 decomposition would introduce a second oxidant.

The illustration in Figure 4 shows the differences in redox conditions established at these two fronts. The value of E_h is the solution redox condition in alpha radiolytically-decomposed water which will vary depending on radiation dose rate. The very positive value of E_h is an indication of the oxidizing potential of H_2O_2 which will control the redox condition at the fuel surface. Providing radiolytically-produced H_2O_2 does not reach the steel, redox conditions at this surface will be established by the water reduction process, for which the equilibrium potential is very low. Consequently, the corrosion processes on the two surfaces will occur at distinctly different E_{CORR} values as illustrated in Figure 4. E_{CORR} for the steel, $(E_{\text{CORR}})_{\text{Fe}}$, will be ≤ -800 mV under anoxic conditions (Blackwood et al. 1995; Smart et al. 2002a, 2002b; Lee et al. 2005) whereas E_{CORR} for the fuel, $(E_{\text{CORR}})_{\text{UO}_2}$, will be > -400 mV if corrosion by radiolytic oxidants is occurring (Figure 2). This large separation introduces the possibility of a number of redox processes between the oxidants produced by radiolysis (H_2O_2), H_2O_2 decomposition (O_2), and fuel corrosion (UO_2^{2+}), and the potential reductants (Fe^{2+} , H_2) formed by steel corrosion. The simplified illustration in Figure 3 suggests the scavenging of oxidants will involve only a series of homogeneous reactions, but the studies to be described below will show this to be a major oversimplification in the case of H_2 .

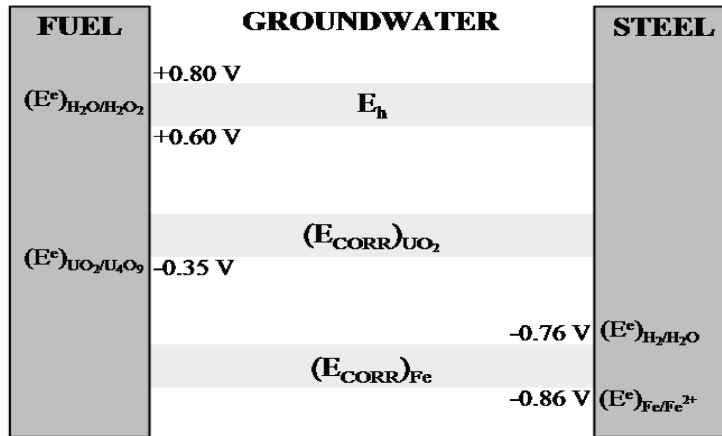
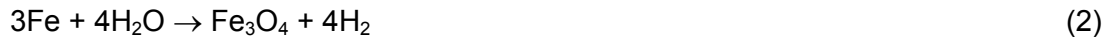


Figure 4: Illustration showing the two corrosion fronts existing within a failed, groundwater-flooded waste container, one on the fuel surface established by reaction with radiolytic oxidants and a second one on the steel surface established by reaction with water. The zone marked E_h indicates the redox condition expected due to the alpha radiolysis of water. The E_{CORR} zones indicate the range of corrosion potentials measured on fuel and steel electrodes.

Under the anoxic conditions anticipated within a failed waste container, carbon steel or iron will react with water to produce Fe^{2+} and H_2 , and the corrosion product magnetite (Fe_3O_4),



Many studies on the influence of Fe and Fe corrosion products on fuel corrosion have been published (Shoesmith et al. 2003; Loida et al. 1996; Grambow et al. 1996; El Aamrani et al. 1998; Loida et al. 2006; Albinsson et al. 2003; Cui et al. 2003; Loida et al. 2001; Quinones et al. 2001; Ollila et al. 2003; Stroes-Gascoyne et al. 2002a, 2002b), and inevitably show that the presence of Fe suppresses corrosion and radionuclide release.

It is not possible to separate the redox-controlling influences of Fe^{2+} and H_2 in experiments involving steel or iron and considerable effort has been expended in studying them separately. Ferrous ion is well known to regulate redox conditions in natural waters (Stumm 1990), and a number of direct attempts have been made to determine the influence of Fe^{2+} and Fe_3O_4 , both experimentally (Quinones et al. 2001; Ollila et al. 2003; Loida et al. 2002; Stroes-Gascoyne et al. 2002a, 2002b) and via model calculations (King and Kolar 2002a, 2002b; Jonsson et al. 2007). The calculations of Jonsson et al. (2007), based on experimentally determined rate constants, indicate that the consumption of H_2O_2 via the Fenton reaction



could suppress UO_2 dissolution by a factor of > 40 .

However, there is a considerable amount of evidence that H_2 has a much larger effect on fuel dissolution than Fe^{2+} . Even relatively small amounts of dissolved H_2 can have a very major influence on fuel corrosion/dissolution, and hydrogen pressures of up to 5 MPa are expected to develop quickly within a failed container (Liu and Neretnieks 2002; Sellin 2001). Consequently, this report will focus on the influence of H_2 on fuel corrosion/dissolution.

3. INFLUENCES OF HYDROGEN ON FUEL CORROSION

A considerable database of information on the influence of H_2 has now been accumulated on a wide range of materials:

- (a) spent fuels, in particular PWR and MOX fuels;
- (b) fuel specimens doped with different quantities of α -emitters to simulate the much lower alpha radiation dose rates expected in spent fuel after long disposal times;
- (c) SIMFUELS, which are unirradiated analogues of used fuel produced by doping UO_2 with a series of stable elements (Ba, Ce, La, Mo, Sr, Y, Rh, Pd, Ru, Nd, Zr) in proportions appropriate to simulate different degrees of reactor burn-up; and
- (d) UO_2 pellets and powder, sometimes incorporating the noble metal Pd.

This information is described and discussed below.

3.1 Spent Fuels

The results of the latest experimental work carried out in a large European research project on spent fuel stability in the presence of H_2 (Poinssot et al. 2005) have recently been reported (Carbol et al. 2005). The early studies in the European program, conducted on high burn-up spent fuel in the presence of powdered Fe and its corrosion products (Grambow et al. 1996) showed that the release rates of all important radionuclides (Sr, Cs, Pu) decreased as the H_2 pressure, from Fe corrosion, in the experimental vessel increased to up to 2.8 bar over the 1,049 days of the experiment. Simultaneously, the dissolution of the UO_2 matrix, taken to be indicated by the rate of release of the Sr inventory in the fuel, appeared to slow down and eventually stop. While this study clearly demonstrated an effect of Fe corrosion on fuel dissolution and radionuclide release it did (could) not separate the influences of Fe^{2+} and H_2 .

To avoid this ambiguity, a further 1,095 day static corrosion experiment was conducted in 5.0 mol/L NaCl under an overpressure of 3.2 bar of H_2 (Carbol et al. 2005). In the early stages of this experiment, when the system was only Ar-purged, the Sr release rate, again used as an indicator of the matrix dissolution rate, was a factor of ~ 14 higher than after the H_2 pressure was eventually applied. This influence of H_2 persisted over the entire subsequent duration of the test during which the solution concentrations of the redox-sensitive radionuclides (Tc, Np, Pu) decreased. The Sr releases rates for this experiment (after H_2 addition) and the original experiment (with Fe powder present) were considerably lower than with only Ar-purging.

To determine whether the aqueous uranium was equilibrating with U^{VI} or U^{IV} solids, the analyzed uranium concentrations were compared to calculated solubilities for UO_2 , and for U^{VI} solids that could feasibly form in the solution used. These calculations were made using the available thermodynamic data-set for U^{IV} and U^{VI} aqueous species and the solids UO_2 , metaschoepite ($UO_3 \cdot 2H_2O$), and sodium diuranate ($NaU_2O_7 \cdot 6H_2O$) (Fanhagel and Neck 2002; Neck and Kim 2001; Neck 2003). For the pressurized H_2 experiment, the measured solubilities were considerably lower than those calculated for U^{VI} solids and essentially coincided with the calculated UO_2 solubility.

For both experiments, analyzed O_2 levels in the reaction vessel were below the detection limit, and E_h values were as low as -500 mV (vs Ag/AgCl) compared to >200 mV when the atmosphere was Ar only. Since a considerable amount of radiolytic O_2 should have been produced at the radiation dose rates present in the fuel specimens, a very efficient scavenging of oxidants must have occurred. The possibility that Fe corrosion by O_2 could account for this scavenging in the first experiment (Grambow et al. 1996) was ruled out by XRD and EDX analyses of the iron corrosion products. Only magnetite (Fe_3O_4) and possibly a small amount of green rust were observed. Magnetite is the expected corrosion product for the anoxic corrosion of iron/steel (Smart et al. 2002a,b) and the traces of green rust is an indication that only very low levels of O_2 could have been present (Lee et al. 2005; Hansen 2002). For the amounts of O_2 calculated to be radiolytically-produced in this experiment, considerable amounts of Fe_2O_3 and α -FeOOH would be expected if the O_2 reacted with the iron (King and Stroes-Gascoyne 2000). The only other available scavenger in both experiments would be H_2 .

A leaching experiment with MOX fuel with a high average burn-up of 48 MWd/KgU (in 10 mM NaCl + 2mM HCO_3^-) showed that the dissolution of even highly α -active fuel could be completely suppressed with a sufficiently high H_2 pressure (53 bar, equivalent to a dissolved H_2 concentration of 4.3×10^{-2} mol/L) (Carbol et al. 2005). No dissolution rate could be calculated since, once the preoxidized layer present on commencement of the experiment had dissolved, no further U release was observed over the 494 days of the experiment. Again, the U concentration approached the solubility of the unoxidized UO_2 matrix, a value of 3×10^{-10} mol/L finally being achieved. The redox-sensitive radionuclides initially released appeared to be reduced and reprecipitated. That no oxide dissolution occurred was strongly supported by the Cs release behaviour. Once the initial Cs release was over (presumably from exposed grain boundaries), no further release was observed over the final 300 days of the experiment.

Such high concentrations of dissolved H_2 are not essential for the suppression of spent fuel corrosion rates. In a flow-through experiment, a decrease in dissolution rate of 3 to 4 orders of magnitude was achieved in the presence of only 8×10^{-4} mol/L of dissolved H_2 (equivalent to a H_2 pressure of about 1 bar) compared to rates measured under oxidizing conditions, Figure 5 (Rollin et al. 2001). By performing a series of experiments as a function of pH (3 to ~ 9.5), it was demonstrated that the rates under oxidizing conditions exhibited the pH dependence expected from controlled laboratory experiments with UO_2 (Torrero et al. 1997; de Pablo et al. 1996; Shoesmith 2000). By contrast, in the H_2 -purged experiments the lack of a pH dependence at low pH (< 6) and the extremely low rates are consistent with a chemical dissolution process. In support of this claim, the measured spent fuel dissolution rates under reducing conditions were shown to be similar to those predicted for potentials around the -400 mV (vs SCE) threshold (Figure 2) below which only chemical dissolution is possible (Shoesmith 2007).

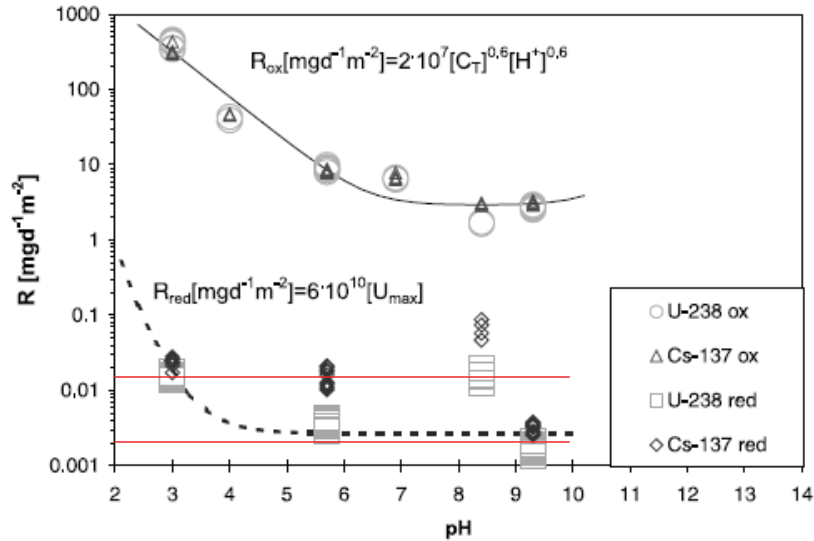


Figure 5: Used fuel dissolution rates as a function of pH for oxidizing and reducing conditions. Oxidizing conditions: solution purged with 20% O₂/0.03% CO₂/ 80% Ar; Reducing conditions, solution bubbled with H₂ containing 0.03% CO₂ over a Pt foil (Rollin et al. 2001). The two horizontal lines are extrapolations of electrochemically measured corrosion rates to -0.35V and -0.45V (Shoesmith 2007).

Many of these observations are consistently observed in other published studies on spent fuel in the presence of H₂ (Grambow et al. 2000; Spahiu et al. 2002, 2004; Ollila et al. 2003), and the key observations can be summarized.

- (i) Despite short-term ambiguities introduced by the presence of preoxidized layers, U concentrations decrease to very low levels with time. The time taken to reach these low levels depends largely on the initial condition of the fuel surface, and how it is treated, either prior to, or during, the initial stages of the experiment.
- (ii) These low U levels are well below the solubilities of U^{VI} solids which could feasibly have deposited in the leaching environment. Comparison of measured U levels to calculated solubilities for UO₂ shows this to be the only solid that could equilibrate with the solution at these concentrations.
- (iii) The concentrations of radiolytically-produced O₂ is generally around or below the detection limit of 10⁻⁸ mol/L, and there is considerable evidence to show these low concentrations are maintained by reaction with H₂ to produce water. At the low temperatures generally employed in spent fuel experiments a reaction between O₂ and H₂ would not be expected to occur in the absence of catalysis by the UO₂ surface.
- (iv) It is dubious as to whether the Sr release rate can be used as an indicator of the fuel dissolution rate. Under oxidizing conditions, when a significant amount of dissolution occurs, the correlation between these rates appears to be good (Grambow et al. 1990;

Loida et al. 2002). However, when only minimal dissolution occurs in the presence of H₂, the release behaviour of Sr appears to be complicated by release of its small grain boundary inventory, which would have been swamped by release from the fuel matrix under oxidizing conditions. In addition, changes in surface properties thought to be induced by its reduction by H₂ may also influence Sr release (Carbol et al. 2005; Spahiu et al. 2004).

- (v) The concentrations of redox sensitive radionuclides decrease throughout the leaching experiments consistent with their reduction and reprecipitation by reaction with H₂.

3.2 Alpha-doped UO₂ Specimens

Since container lifetimes are expected to be long, spent fuel is unlikely to be exposed to groundwater over the 300 to 1,000 year period over which γ/β radiation fields are significant, Figure 1. Beyond this period, α -radiation fields will dominate and be the source of oxidants for fuel corrosion via the α -radiolysis of water. To study the influence of α -radiation without interference from γ/β fields, α -doped UO₂ specimens have been used. These specimens contain different fractions of α -emitters (²³⁸Pu, ²³³U) to simulate the levels of α -activity in spent fuels after various periods of containment (Poinssot et al. 2005; Carbol et al. 2005; Stroes-Gascoyne et al. 2002a,b; Stroes-Gascoyne and Betteridge 2005). Based on studies with α -emitters and a number of spent fuel studies, a dependence of fuel corrosion rate on α -activity is now well established, Figure 6, and has been discussed in detail (Poinssot et al. 2005).

Experiments performed with ²³³U-doped UO₂ (1% and 10% ²³³U) in a carbonate-dominated water ($\sim 10^{-3}$ mol/L, pH = 7.5) containing no H₂ showed no measureable influence of α -radiation at the 1% doping level (over 46 days) suggesting the alpha activity of this specimen represents an approximate threshold below which solubility-controlled, as opposed to radiolytically-controlled, dissolution would prevail, as suggested by Poinssot et al. (2005) and indicated by the break in the dashed lines in Figure 6. The rates measured at this threshold are very similar to those predicted using a simple extrapolation of electrochemical data (Shoosmith and Sunder 1991) to the E_{CORR} threshold shown in Figure 2. This consistency adds credibility to the claim that a threshold does exist and can be used to interpret the influence of H₂ on fuel dissolution rate. A repeat of these experiments in the presence of an Ar/6% H₂-purge (equivalent to a H₂ concentration of 5×10^{-5} mol/L) showed that even this small concentration of H₂ suppressed the dissolution rate below this threshold; i.e., no U release was observed with the 1% ²³³U-doped UO₂ sample.

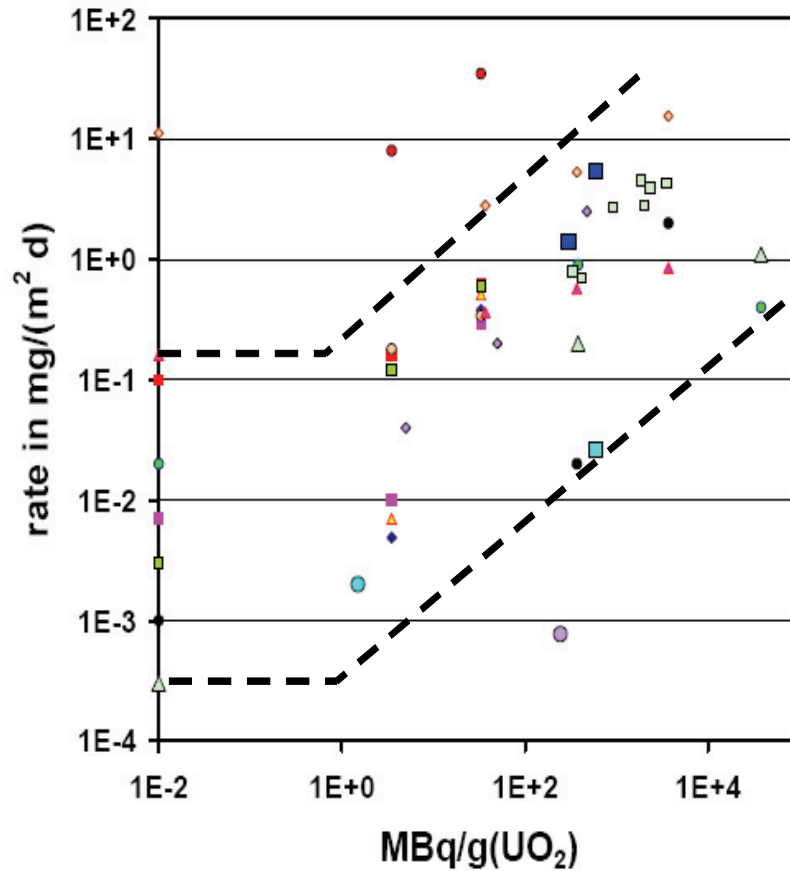


Figure 6: Corrosion rates measured for alpha-doped UO_2 , non-doped UO_2 (0.01 MBq/g) and spent fuel specimens as a function of alpha activity (Poinssot et al. 2005). The sources of the individual data points are given in the reference. The dashed lines are arbitrary and drawn to emphasize the approximate alpha-strength below which no influence of alpha radiation is observed (1 MBq/g).

Subsequently, using the 10% ^{233}U -doped UO_2 an experiment was conducted in a solution containing 2×10^{-3} mol/L NaCl and 2×10^{-3} mol/L HCO_3^- in which the H_2 pressure was varied in stages from an initial value of 16 bar (about 10^{-2} mol/L dissolved H_2) to a final value of 0.01 bar (10^{-5} mol/L dissolved H_2) (Carbol et al. 2005). All the indicators that corrosion/dissolution were completely suppressed were observed, Figure 7.

- (i) The U concentration was extremely low ($\leq 10^{-10}$ mol/L), indicating solubility-control over the full 2.2 years of the experiment.

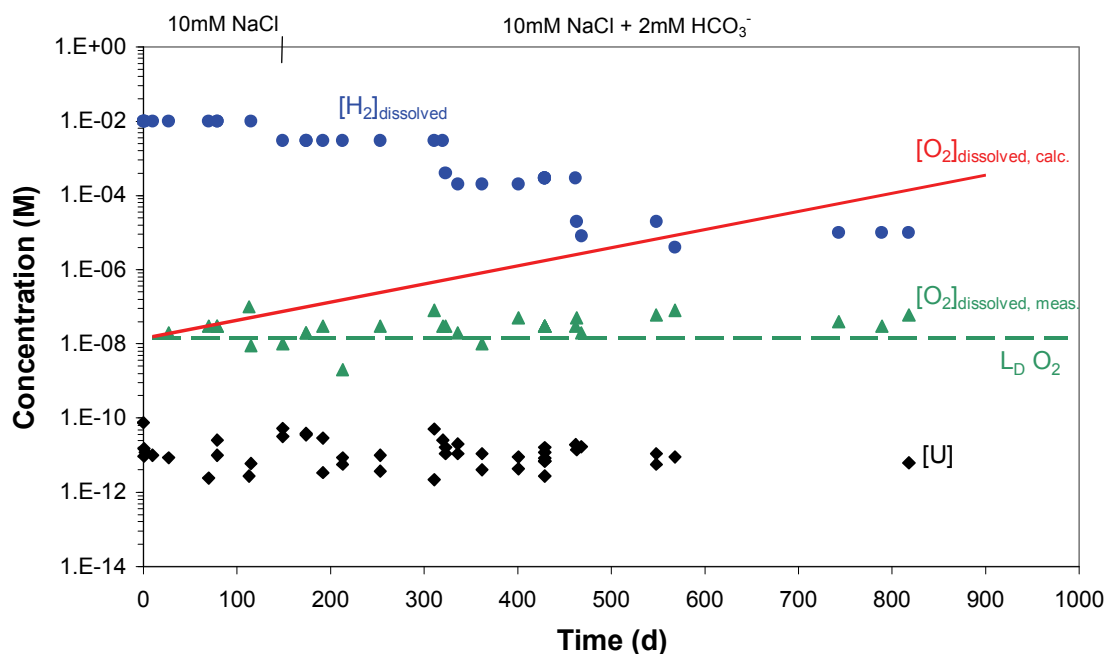


Figure 7: Measured H₂, O₂ and total U concentrations, as a function of time, in a pressure vessel leaching experiment of a 10% ²³³U-doped UO₂ in 10⁻² mol/L NaCl (0 to 114 days) and 10⁻² mol/L NaCl + 2 x 10⁻² mol/L HCO₃⁻ (114 days onwards) as the H₂ overpressure was periodically changed. The red line shows the calculated radiolytic O₂ concentrations (Carbol et al. 2005).

- (ii) The E_h, initially -100 mV (vs SHE), decreased over the first 50 days to ≤ -300 mV and remained well below -300 mV thereafter, only rising over the final days of the last period when the H₂ concentration was at its lowest. This final increase was not accompanied by an increase in U concentration, indicating that reducing conditions were maintained at the fuel surface even at this very low final H₂ concentration.
- (iii) Measured O₂ concentrations were in the region of 10⁻⁸ mol/L throughout the experiment, even though the amount of radiolytically-produced O₂ should have been many orders of magnitude greater by the end of the experiment.
- (iv) The absence of any surface oxidation of the UO₂ was confirmed by X-ray photoelectron spectroscopy (XPS). Also, although the presence of UO₂ fragments in the vessel made analyses somewhat ambiguous, there was no evidence for the redeposition of dissolved U.

Since no change in U concentration occurred over the full two years of the experiment, no dissolution rate could be calculated and it could be concluded that dissolution had been completely suppressed.

This conclusion is strongly supported by the XPS results, which are consistent with previous XPS analyses of UO₂ surfaces exposed to radiation under Ar-purged and H₂-purged (0.1 to 1 bar) conditions (Sunder et al. 1990). These authors showed that, in the absence of radiation at 100°C the extent of oxidation of a UO₂ surface was the same in the presence of H₂ as it was in an Ar-purged system. However, when the UO₂ (a disc cut from a CANDU fuel pellet) was placed close to a ²⁴¹Am source, surface oxidation occurred in Ar-purged solution, but in the presence of H₂, the extent of oxidation of the UO₂ surface decreased as the α -source strength increased.

These results were qualitatively confirmed by the dissolution rates determined electrochemically (by a standard Tafel extrapolation and by electrochemical impedance spectroscopy (EIS)) (Carbol et al. 2005), which showed a dependence of dissolution rate on α -activity and a suppression of the rate for both 1% ²³³U and 10% ²³³U electrodes in the presence of H₂. These rates are included in Figure 6, and are high compared to other rates; i.e., outside the area encompassed by the dashed lines. This probably reflects the difficulties inherent in making EIS measurements on an electrode with a bulk resistance of 10⁵ ohms.

Given the absence of any UO₂ corrosion the lack of radiolytic oxygen cannot be attributed to its consumption by fuel corrosion, leaving its consumption by H₂ catalyzed by the fuel surface as the only alternative explanation.

3.3 The Role of Gamma Radiation in the Activation of H₂

It is clear from these studies on spent fuels and α -doped specimens that dissolved H₂ can suppress fuel corrosion completely, even at low concentrations. Also, H₂ can reduce the concentrations of radiolytic oxidants down to their analytical detection limits. At the low temperatures employed it has been shown that H₂ cannot act as a homogeneous solution reductant; e.g., for U^{VI} (Spahiu et al. 2004), Np^V (Cui and Eriksen 1996) and Tc^{VII} (Guppy et al. 1989). To act as a reductant H₂ must be activated; i.e., dissociated into reactive H atoms, a process that can be achieved either radiolytically or on catalytic surfaces. For the present systems a combination of these two modes is possible.

The homogeneous activation of H₂ by low energy transfer (LET) radiation, which generates OH[•] radicals, to produce reactive hydrogen radicals



has been demonstrated computationally (Tait and Johnson 1986) and experimentally (Pastina et al. 1999, 2001). H₂ concentrations in the range found to suppress fuel corrosion (10⁻⁴ to 10⁻⁵ mol/L) have been shown to scavenge molecular radiolytic oxidants to below detection limits as well as consume small amounts of added H₂O₂. While this can readily explain the scavenging of radiolytic oxidants in spent fuel experiments, it is insufficient to explain the complete absence of fuel dissolution, as well as a number of other laboratory observations made on UO₂ electrodes exposed to gamma irradiated solutions.

King et al. (1999) studied the effect of γ -radiation on the E_{CORR} of UO₂ (CANDU) in the presence of either a 5 MPa over pressure of H₂ (equivalent to ~ 4 x 10⁻² mol/L of dissolved H₂) or Ar. A comparison of the E_{CORR} values obtained under irradiation in the presence of H₂ to the values in the presence of Ar is shown in Figure 8. The range of values recorded in unirradiated solutions

for both gases are shown as a vertical bar (King and Shoesmith 2004). Under irradiation, E_{CORR} values in the presence of H_2 were consistently more negative, and those in the presence of Ar consistently more positive, than values measured in the absence of radiation. This increase in E_{CORR} in Ar is expected due to a slight radiolytic oxidation of UO_2 when a radiation field is present.

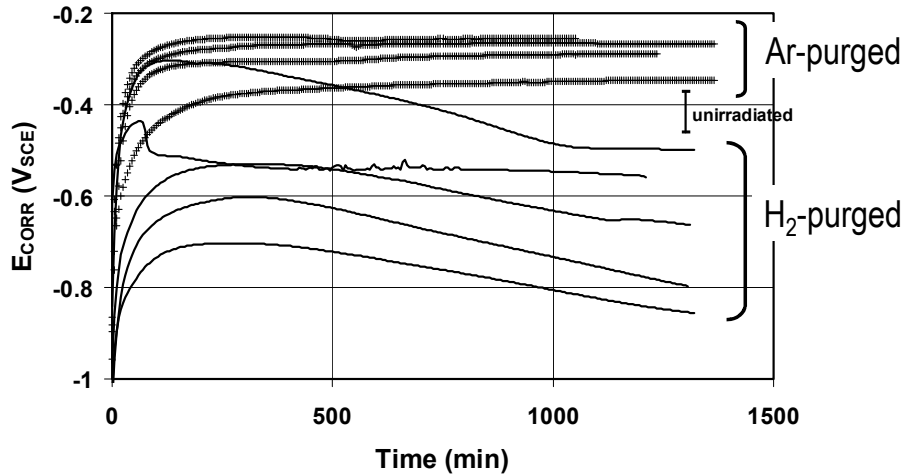


Figure 8: Time dependence of the corrosion potential (E_{CORR}) of a UO_2 electrode in gamma-irradiated 0.1mol/L NaCl (pH~9.5) at room temperature in the presence of either 5MPa of H_2 or Ar. The results of four or five replicate tests are shown for each set of conditions. The range of E_{CORR} values recorded in unirradiated solutions for both gases is shown as the vertical bar (King and Shoesmith 2004).

However, the influence of H_2 is more dramatic than can be explained by just the homogeneous solution scavenging of radiolytic oxidants. Comparison of the absolute values in Figure 8 with the threshold potential for surface oxidation of UO_2 , Figure 2, shows that E_{CORR} is suppressed to values up to 400 mV more negative than the threshold for oxidation/corrosion, and approaches the reversible potential for the reaction



which proceeds on surfaces through reactive H^\bullet radical intermediates. A general observation in these experiments is the peak in the E_{CORR} versus time relationship in the presence of H_2 , the decrease in E_{CORR} at longer times suggesting that the state of the UO_2 surface is slowly changing. Since the electrodes were pre-treated electrochemically to remove air-formed U^{VI} oxides, this change cannot be attributed to the reduction of a pre-oxidized surface layer. The most probable, but unproven, explanation is that γ -assisted decomposition of H_2 produces H^\bullet radicals which subsequently reduce U^V surface states, present in residual slightly non-stoichiometric sites, to U^{IV} ,



This surface reduction appears to be partially irreversible as shown in Figure 9, which shows the E_{CORR} response to changes in the pressurizing gas during the experiment. The critical observation in these experiments is that, after exposure to H_2 , E_{CORR} does not recover to the value measured on first exposure to an Ar purge, suggesting that the UO_2 surface may have been permanently reduced by radiolytically-produced H^\bullet radicals on the surface.

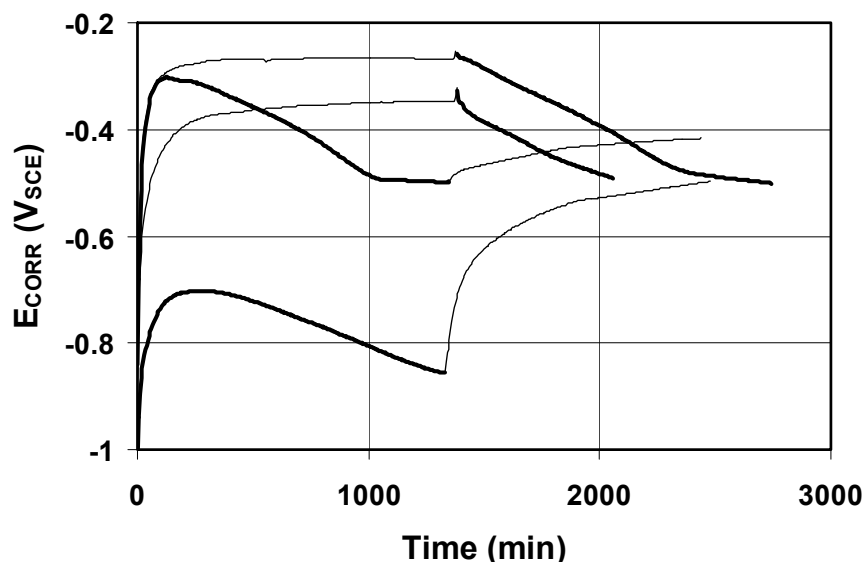


Figure 9: Effect of changing from H_2 (heavy line) to Ar (light line) overpressure on the E_{CORR} of UO_2 in γ -irradiated $0.1 \text{ mol}\cdot\text{dm}^{-3}$ NaCl solution (pH 9.5) at room temperature (King et al. 1999).

A surface reduction step, as described in reaction 7, must simultaneously involve the extraction of an interstitial O^{2-} ion from the $(\text{U}^{\text{IV}})_{1-2x}(\text{U}^{\text{V}})_{2x}\text{O}_{2+x}$ lattice in order to maintain electrical neutrality in the surface. This would likely be achieved by consumption of the proton produced. Consequently, a reduction reaction of this type can be considered as a defect annealing process since the primary defect in slightly non-stoichiometric UO_{2+x} is the O^{2-} interstitial ion occupying vacancies in the UO_2 fluoride structure (Shoosmith et al. 1994).

For gamma radiation it is also feasible that enhanced radiolytic effects at the oxide/solution interface involving the creation of excitons is involved (Petrik et al. 2001). Excitons are produced by the absorption of radiation in the solid. Providing the oxide band gap is sufficiently large (5 eV) that these excitons have sufficient energy to break H-O-H bonds (5.1 eV), they can act as a source of OH^\bullet and H^\bullet radicals. Reaction of the OH^\bullet radical with H_2 would create an additional H^\bullet radical,



These H^\bullet radicals can scavenge radiolytic oxidants and suppress fuel oxidation/corrosion. In the reduced state, when the 5f level is fully occupied, UO_2 does possess the 5 eV band gap which allows formation of the high energy excitons.

3.4 The Role of Alpha Radiolysis in the Activation of H₂

While this combination of γ -radiolysis and γ -activation of H₂ on the UO₂ surface offers an explanation for the scavenging of radiolytic oxidants and suppression of radiolytic corrosion of spent fuels, it cannot explain the similar results obtained with α -doped specimens when γ/β radiation fields are absent. In the case of α -radiation, it has been shown (Pastina and Laverne 2001) that even quite large amounts of H₂ (up to 1 bar, equivalent to 8×10^{-4} mol/L) did not influence the production of radiolytic oxidants in the absence of UO₂. Practically equal amounts were produced with and without H₂, in solutions irradiated with 5 MeV He atoms. Also, while radiolysis models developed for spent fuels show that the combination of $\gamma/\beta/\alpha$ radiation and H₂ can lead to the consumption of radiolytically-produced molecular oxidants (Eriksen 1996; Jonsson et al. 2003; Grambow et al. 2004), the continuous generation of molecular oxidants by α -radiolysis means conditions remain locally oxidizing even at high H₂ pressures. Thus, no argument can be made that the homogeneous solution scavenging of radiolytic oxidants alone can completely suppress radiolytic corrosion of UO₂.

Thus, a surface activation of H₂ to produce reactive H^{*} radicals similar to that observed in the presence of γ -radiation must be available on α -doped UO₂ surfaces. Evidence exists to show that H₂ and O₂ can be recombined on α -active ²³⁹PuO₂ surfaces at 25°C (Haschke et al. 1996). In addition, radiolytic H₂ gas generation via the decomposition of water on NpO₂ (doped with the α -emitter ²⁴⁴Cm) achieves a steady-state indicative of a balance between H₂O decomposition and the reverse H₂/O₂ recombination process. A similar mechanism can be anticipated on α -doped UO₂ even though no water production was detected in an H₂/O₂ mixture on depleted UO₂ (which would have effectively negligible α -activity (Devoy et al. 2003)).

Catalysis on UO₂ surfaces is well characterized and catalytic activity is considerably enhanced on defective surfaces. Defective surfaces can be created by Ar ion sputtering which, for an actinide oxide like UO₂, leads to preferential ejection of the much lighter O atom and the creation of an oxygen vacancy. The need to repair this site can lead to the extraction of oxygen from, and hence the reduction of, absorbed species. The actinide oxides are particularly reactive, especially U, since hybridization between the 5f and 6d electronic orbitals allow the creation of multiple oxidation states (+3 to +6) in the solid state. These features have led to uranium oxides being studied for the catalysis of many reactions including dehydrogenation (Madhavaram and Idriss 1999), oxidation (Taylor et al. 2000; Heneghan et al. 1999), ammoxidation (Graselli et al. 1981; Graselli and Suresh 1972), oxidative coupling (Madhavaram and Idriss 2002) and etherification (Ai 1983). Most pertinent to the present discussion is the demonstration that water decomposition involving the oxidative healing of defects in the reduced surface occurs on UO₂ and is promoted when the surface defect density is increased by Ar ion sputtering (Senanyake et al. 2007). Alpha emission will also produce surface defects by the preferential ejection of the lighter O atom leading to reduced (U^{III}) states. Subsequent oxidation of the surface by H₂O, leading to the reincorporation of O²⁻, would yield a proton and leave an H^{*} available to scavenge radiolytic oxidants. This provides one possible mechanism by which radiolytic oxidants can be consumed at the location they are produced for as long as α -radiolysis persists and H₂ is present.

3.5 The Role of Noble Metal (Epsilon [ϵ]) Particles in the Control of Surface Redox Conditions

In-reactor irradiation has a significant influence on the chemical and physical properties of the fuel due to the production of a wide range of radionuclides (Kleykamp 1985, 1988; Johnson et al. 1988). Of key importance from the present perspective are the rare earths (RE) (e.g., Nd, Eu, Gd) which reside in the fuel lattice as RE^{III} cations and create additional U^V species leading to an increase in matrix electrical conductivity (Shoesmith et al. 1994), and the elements which are unstable as oxides (Mo, Ru, Pd, Rh, Tc), which segregate to form noble metal particles known as ϵ -particles.

Noble metals are well known as catalysts for oxidation/reduction reactions, especially the H₂/H^{*}/H⁺ reaction, and three of the four predominant components of ϵ -particles (Rh, Pd, Ru) are exceptionally good catalysts for this reaction as evidenced by their exchange current densities, Table 1 (Broczkowski 2008; Norskov et al. 2005).

Table 1: Exchange current densities for the proton reduction reaction for the four predominant epsilon particle constituents

Element	Exchange Current Densities (A.cm ⁻²)
Pd	10 ^{-3.0}
Rh	10 ^{-3.6}
Ru	10 ^{-3.3}
Mo	10 ^{-7.1}

Thus, it would be expected that these particles could act as galvanically-coupled anodes (for H₂ oxidation) and cathodes (e.g., for H₂O₂ reduction). Thus, H₂ activation on these particles is likely to be at least as effective in suppressing fuel corrosion as the utilization of defects produced by α -recoil or the γ -excitation of H₂ (Cui et al. 2004; Nilsson and Jonsson 2007; Shoesmith 2007). The function of these particles has been investigated electrochemically using SIMFUEL specimens with different degrees of simulated burn-up (Broczkowski et al. 2005, 2006, 2007; Broczkowski 2008). SIMFUELS are unirradiated analogues of used nuclear fuel, produced by doping the UO₂ matrix with a series of stable elements (Ba, Ce, La, Mo, Sr, Y, Rh, Pd, Ru, Nd and Zr) in proportions appropriate to simulate the chemical effects caused by in-reactor irradiation to various levels of burn-up. This fabrication process reproduces the increase in matrix conductivity due to RE dopants and the creation of noble metal particles.

Figure 10 shows the distribution of epsilon particles for three SIMFUELS with various degrees of simulated burn-up covering the range from the level expected in CANDU fuel (1.5 at %) to that expected for a very high burn-up enriched fuel (6 at %). This distribution was obtained from SIMS analysis for the individual elements in the particles. The increase in size and number density of particles with the increase in degree of simulated burn-up is clear.

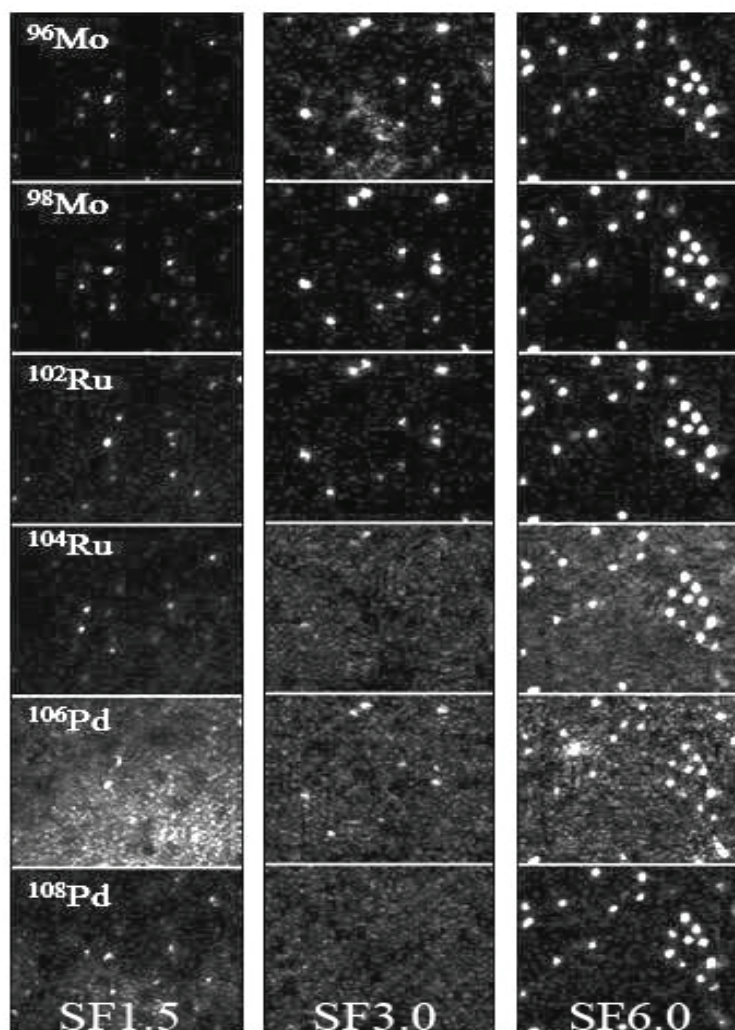


Figure 10: SIMS images showing the elements $^{96,98}\text{Mo}$, $^{102,104}\text{Ru}$, and $^{106,108}\text{Pd}$ detected in three SIMFUEL specimens (SF) with various degrees of simulated burn-up (expressed as an atomic %). No map for Rh is shown due to its low concentration. Each individual area is $50\ \mu\text{m} \times 50\ \mu\text{m}$.

The E_{CORR} on SIMFUELS is very responsive to variations in redox conditions, Figure 11. In the presence of dissolved O_2 (aerated solutions) oxidation of the fuel surface is catalyzed by O_2 reduction on the ϵ -particles. A similar catalysis of H_2O_2 reduction occurring on Pd particles dispersed throughout UO_2 was also demonstrated to cause enhanced corrosion (Nilsson 2008). However, the presence of even small amounts of dissolved H_2 (purging with 5% $\text{H}_2/95\%$ Ar) suppressed E_{CORR} well below the value measured under purely anoxic conditions (Ar-purging) even for a low density of ϵ -particles (1.5 at % SIMFUEL, Figure 11).

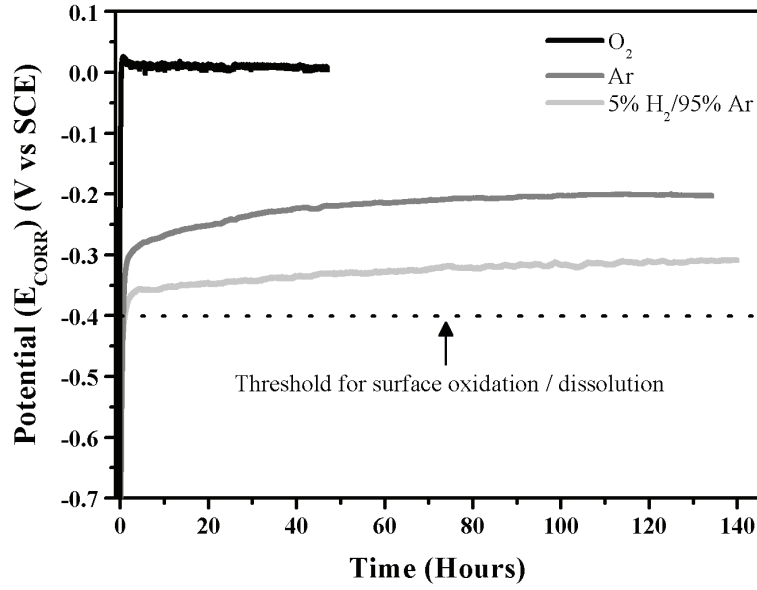


Figure 11: E_{CORR} measurements on a SIMFUEL electrode (SF1.5, with an extent of simulated burn-up of 1.5 at %) in a 0.1 mol/L KCl solution (pH = 9.5) purged with various gases at 60°C. The electrode was electrochemically-cleaned prior to the start of each experiment. The dashed line shows the potential threshold for corrosion (Figure 2) (Broczkowski et al. 2005).

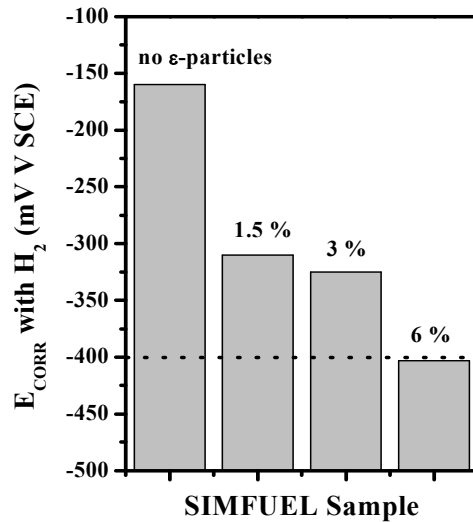


Figure 12: The influence of the increasing number and size of epsilon particles in SIMFUELS with different degrees of simulated burnup (expressed as an atomic %) on the corrosion potential (E_{CORR}) measured in H_2 -purged 0.1mol/L KCl solution (pH = 9.5) at 60°C. The horizontal line shows the potential threshold for corrosion (Figure 2) (Shoesmith 2007).

The value of E_{CORR} decreased with the number density of ϵ -particles present, Figure 12, and XPS analyses confirmed that the extent of oxidation of the UO_2 surface decreased as E_{CORR} decreased, Figure 13.

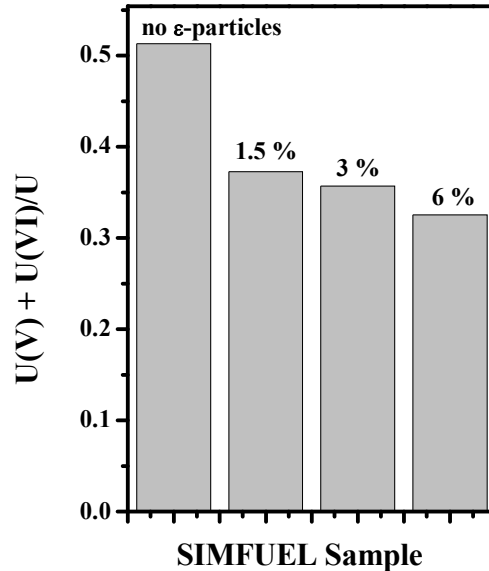


Figure 13: The influence of the increasing number and size of epsilon particles in SIMFUELS with different degrees of simulated burnup (expressed as an atomic %) on the degree of oxidation of the surface (determined by XPS) in H_2 -purged 0.1mol/L KCl (pH = 9.5) at 60°C . The horizontal line shows the potential threshold below for corrosion (Figure 2) (Shoesmith 2007)

For the 6 at % SIMFUEL, with a high number density of ϵ -particles, E_{CORR} was suppressed to a value of -400 mV (vs SCE), the threshold below which corrosion of UO_2 does not occur. This effect can be attributed to the reversible dissociation of H_2 to H^\bullet radicals on the ϵ -particles that act as galvanically-coupled anodes within the fuel matrix. When E_{CORR} reaches, or is suppressed below, this threshold, the UO_2 is fully galvanically protected and thermodynamically immune to corrosion. This process is illustrated schematically in Figure 14. That immunity to oxidation, and hence corrosion, is achieved is confirmed by the XPS analyses which show that the surface composition is as reduced as that achieved by electrochemical reduction of the electrode at potentials < -1 V (vs SCE) (Broczkowski 2008).

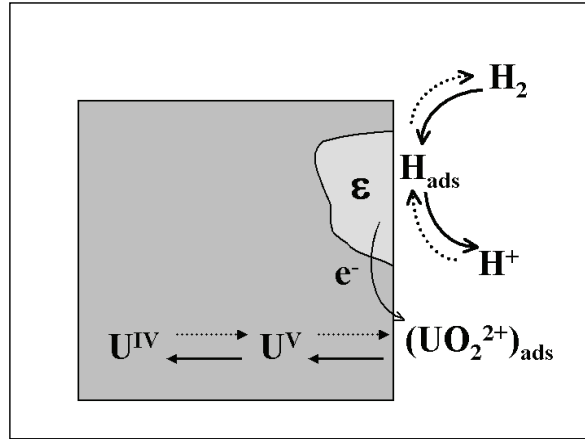


Figure 14: Illustration showing the galvanic coupling of epsilon particles to the fuel matrix in H_2 -containing solutions (Broczkowski et al. 2005).

Measurements performed in a pressure vessel show that E_{CORR} can be suppressed well below the threshold even on 1.5 at % SIMFUEL, providing the pressure of H_2 is increased sufficiently, Figure 15. It is worth noting that the potential achieved under these conditions approaches the reversible potential for the $H_2/H^+/H^+$ reaction as observed on UO_2 containing no ϵ -particles in the presence γ -radiation, Figure 8. For this condition, the $H_2/H^+/H^+$ reaction becomes reversible on the ϵ -particles and the UO_2 matrix is completely inert.

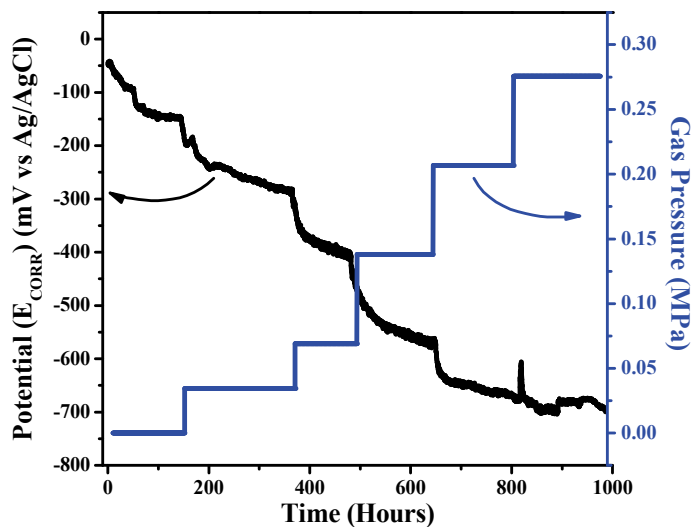


Figure 15: The influence of H_2 solution overpressure on the E_{CORR} of a SIMFUEL electrode with 1.5% of simulated burn-up (SF1.5) measured in a 0.1 mol/L KCl solution (pH = 9.5) at $60^\circ C$. The system was initially purged with Ar only at atmospheric pressure, and then with a series of increasing 5% H_2/Ar pressures (Broczkowski et al. 2005).

Since noble metals are catalytic for both the reduction of potential fuel oxidants, such as H_2O_2 , as well as the reductant H_2 , it is not surprising that it can be shown that ϵ -particles will catalyze the reaction between H_2O_2 and H_2 to produce water; i.e., ϵ -particles will catalyze the scavenging of radiolytic oxidants by H_2 . Nilsson and Jonsson (2007) showed that Pd, present as a powder, acted as a catalyst for this reaction and Broczkowski has shown that a similar catalysis occurs on the ϵ -particles in 1.5 at % SIMFUEL (Broczkowski 2008). The reaction was shown to be diffusion controlled on Pd which could account for the very strong effect of H_2 on spent fuel dissolution at very modest concentrations (10^{-5} to 10^{-4} mol/L) (Carbol et al. 2005).

Figures 16 and 17 show the E_{CORR} response of a 1.5 at % SIMFUEL surface to the addition of small concentrations of H_2O_2 under Ar-purged conditions, Figure 16, and with a 5% H_2 /95% Ar purge ($\sim 4.5 \times 10^{-5}$ mol/L of dissolved H_2), Figure 17. In the absence of H_2 , E_{CORR} increases to a new steady-state value which increases with increasing H_2O_2 concentration, and XPS analyses show that the extent of oxidation of the surface increases accordingly (Broczkowski 2008). The addition of similar concentrations of H_2O_2 in the presence of H_2 initially stimulated an increase, but eventually a decrease, in E_{CORR} for sufficiently low H_2O_2 concentrations. Note the steady-state E_{CORR} in this experiment prior to H_2O_2 addition is lower than that in the Ar-purged solution (Figure 16), which reflects the dissociation of H_2 on the ϵ -particles and its galvanically-coupled effect on the UO_2 .

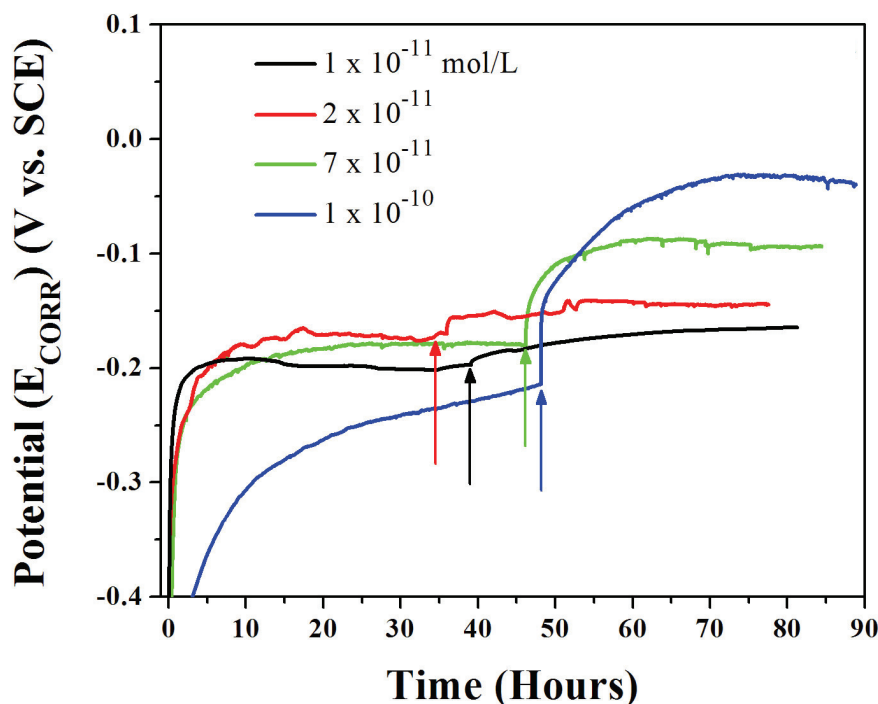


Figure 16: E_{CORR} recorded on a SIMFUEL with 1.5% of simulated burn-up (SF1.5) in a $0.1 \text{ mol}\cdot\text{L}^{-1}$ KCl solution (pH 9.5) purged with Ar at 60°C . The arrows indicate the times when H_2O_2 was added in the individual experiments (Broczkowski 2008).

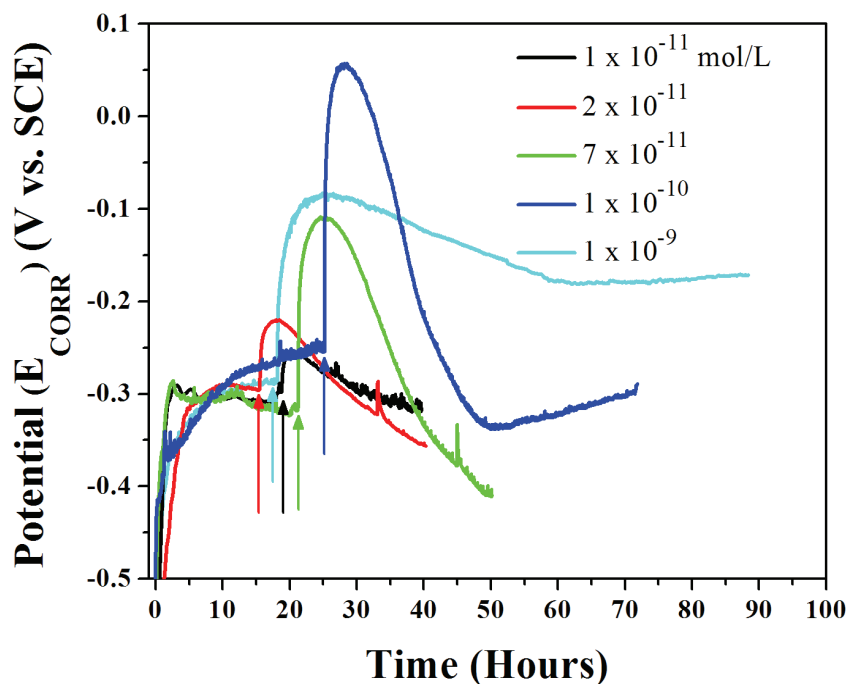


Figure 17: E_{CORR} recorded on a SIMFUEL with 1.5% of simulated burn-up (SF1.5) in a $0.1 \text{ mol}\cdot\text{L}^{-1}$ KCl solution (pH 9.5) purged with 5% H_2 /95% Ar at 60°C . The arrows indicate the times when H_2O_2 was added in the individual experiments (Broczkowski 2008).

XPS analyses confirm that no permanent oxidation of the surface occurred except at a H_2O_2 concentration of 10^{-9} mol/L , when E_{CORR} did not fully recover to the value measured prior to H_2O_2 addition, Figure 18. In this figure the lines indicate the $\text{U}^{\text{IV}}/\text{U}^{\text{V}}/\text{U}^{\text{VI}}$ levels in the UO_2 surface under H_2 -purged conditions (i.e., before H_2O_2 addition) and the data points show the surface composition after the addition of H_2O_2 and completion of E_{CORR} excursions similar to those shown in Figure 17.

This E_{CORR} behaviour cannot be attributed solely to H_2O_2 scavenging by H_2 on ϵ -particles, independently of the galvanic coupling effect. While it is possible that the positive excursion in E_{CORR} lead to a temporary oxidation of the UO_2 surface, the XPS results demonstrate that this was not sustainable. Irrespective of whether the H_2O_2 was eventually consumed in these experiments, the absence of UO_2 oxidation confirms that galvanic protection of the UO_2 was maintained or eventually reestablished. In fact, the XPS analyses suggest the UO_2 surface is actually reduced to a level below its original composition, Figure 18.

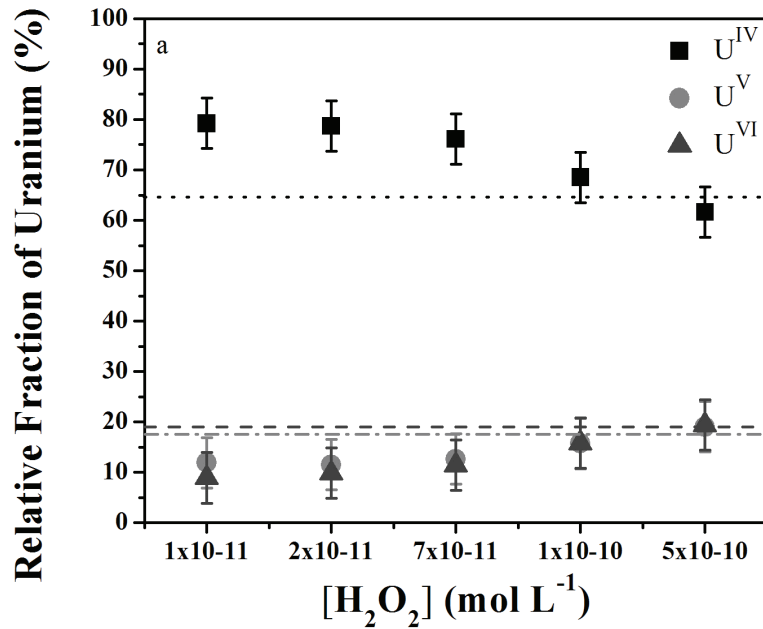
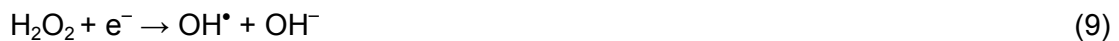


Figure 18: Surface composition measured (by XPS) on a SIMFUEL with 1.5% of simulated burn-up (SF1.5) after E_{CORR} measurements in 5% H₂/95% Ar-purged 0.1 mol/L KCl solution (pH = 9.5) at 60°C. The horizontal dotted lines refer to the fraction of U^{IV} (black), U^V (light grey), and U^{VI} (dark grey) measured after E_{CORR} experiments with no H₂O₂ added (Broczkowski 2008).

3.6 The Role of the UO₂ Surface in the Control of Surface Redox Conditions

A remaining question is whether or not the UO₂ surface itself can activate H₂ in the absence of ϵ -particles and/or radiation fields. Wren et al. (2005) claimed that a U_{1-2x}^{IV}U_{2x}^VO_{2+x} surface could catalyze the reaction between H₂ and H₂O₂ based on the slow rate of oxidation of UO₂ surfaces in close proximity to an Au-plated ²⁴¹Am α -source. These experiments were conducted in 0.1 mol/L NaClO₄ (pH = 9.5) solutions at room temperature. The oxidation rate was up to two orders of magnitude lower in the presence of α -radiolysis than when H₂O₂ was added chemically and approximately one order of magnitude lower than oxidation by the considerably slower oxidant, O₂. It was speculated that the surface catalyzed decomposition of H₂O₂



proceeded through a OH^\bullet surface species which could subsequently be consumed by α -radiolytically produced H_2 confined in the $25\ \mu\text{m}$ thick layer of solution separating the UO_2 and Au-plated α -source,



However, Nilsson and Jonsson (2008) could find no evidence for this reaction in a system containing $2 \times 10^{-4}\ \text{mol/L}$ H_2O_2 and up to 40 bar of H_2 ($\geq 2 \times 10^{-2}\ \text{mol/L}$ of dissolved H_2). Additionally, the observation that H_2 will reduce UO_2^{2+} when Pd is present (Nilsson et al. 2008), but not when UO_2 alone is present (Ekeröth et al. 2004), also suggests the UO_2 surface cannot activate H_2 .

That H_2 cannot be activated, or activated only to a minor degree, on UO_2 appears to be confirmed by the results in Figure 19, in which the influence of an increase in H_2 pressure on E_{CORR} measured on a rare-earth doped SIMFUEL without ϵ -particles is shown (Broczkowski 2008). As opposed to measurements on SIMFUEL with ϵ -particles, when E_{CORR} was suppressed to values well below the $-400\ \text{mV}$ threshold value for UO_2 oxidation/corrosion, Figure 15, E_{CORR} showed only a minor change with increasing H_2 pressure indicating no significant change in the properties of the surface had occurred.

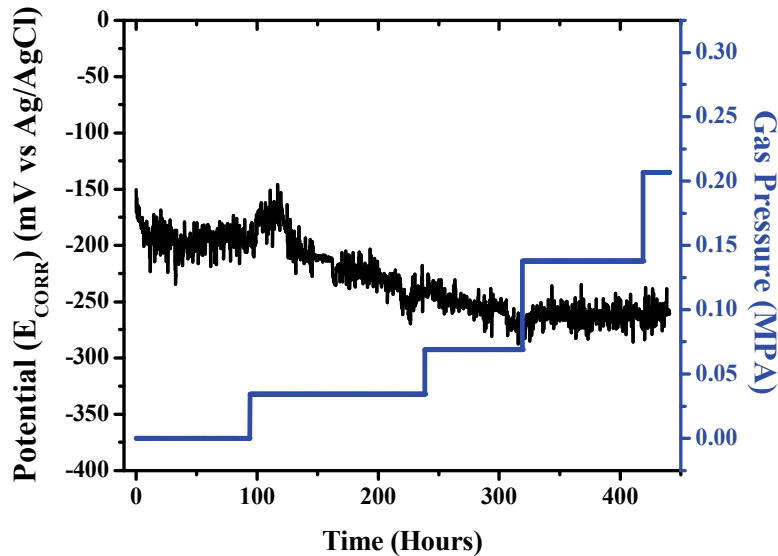


Figure 19: The influence of H_2 overpressure on the E_{CORR} of a SIMFUEL electrode with 3.0% simulated burn-up, but containing no epsilon particles, in a $0.1\ \text{mol/L}$ KCl solution ($\text{pH} = 9.5$) at 60°C . The system was initially purged with Ar only at atmospheric pressure, and then with a series of increasing 5% H_2/Ar pressures (Broczkowski et al. 2005).

However, a series of experiments in which small additions of H_2O_2 were made to 5% $\text{H}_2/95\%$ Ar-purged solutions showed that the E_{CORR} measured on the SIMFUEL with no ϵ -particles exhibited similar behavior, Figure 20, to that observed for the 1.5 at % SIMFUEL, Figure 16. The rapid increase in E_{CORR} on first adding the H_2O_2 was reversed, as observed when ϵ -particles were present. This reversal in E_{CORR} suggests the H_2O_2 is being consumed by reaction with H_2 on the UO_2 surface. Unfortunately, although XPS analyses showed slight differences between the electrodes exposed to either Ar-purged or H_2/Ar -purged solutions, the differences were too small to indicate a clear difference in composition.

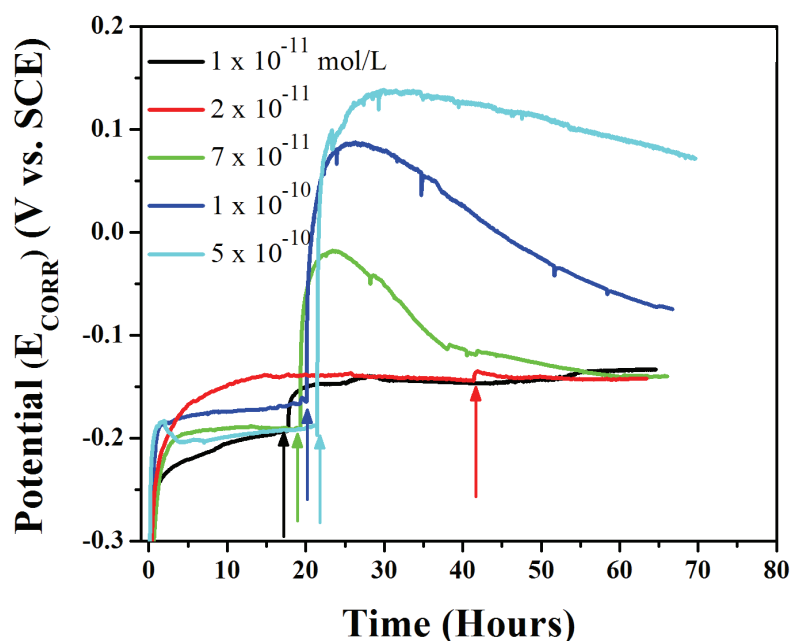


Figure 20: E_{CORR} measured on a SIMFUEL with 3 at % simulated burn-up, but containing no epsilon particles in a 0.1 mol/L KCl solution (pH 9.5) purged with 5% $\text{H}_2/95\%$ Ar at 60°C. The arrows indicate the times when H_2O_2 was added in the individual experiments (Broczkowski 2008).

However, the results strongly suggest that, while H_2 may not dissociatively absorb on UO_2 , H_2O_2 does, and that the $\cdot\text{OH}$ radical species formed can then be scavenged by H_2 leading to H_2O_2 consumption rather than fuel oxidation. Good electrochemical evidence exists to show that the first electron transfer to H_2O_2 involves the creation of an OH^\cdot radical (Goldik et al. 2005, 2006). The results in Figure 20 show that, for this scavenging process to occur, the concentration ratio $[\text{H}_2]/[\text{H}_2\text{O}_2]$ needs to be $>10^5$. This may explain why a similar effect was not observed by Nilsson and Jonsson 2008 since their concentration ratio was only $\sim 10^2$.

It can be concluded that the scavenging of low concentrations of radiolytic oxidants would occur on the UO_2 surface in the presence of a sufficient H_2 concentration. However, the process

appears to be kinetically slow when compared to the reaction rate on ϵ -particles or when H_2 is radiolytically activated.

4. SUMMARY AND CONCLUSIONS

The results of corrosion/dissolution studies on spent fuels, α -doped UO_2 specimens, SIMFUELS and undoped UO_2 specimens have been reviewed, and the mechanisms proposed to explain the ability of dissolved H_2 to completely suppress fuel corrosion and radionuclide release discussed.

The primary reductant leading to the protection of the fuel against corrosion is the H^\cdot radical species which can be produced by a number of activation steps depending on the composition of the fuel and the form of the radiation present. The potential mechanisms include the following:

- (i) A combination of γ -radiation and dissolved H_2 can produce H^\cdot radicals on the UO_2 surface. This may involve the adsorption of γ energy in the surface to produce high energy excitons which decompose water to OH^\cdot and H^\cdot surface species. Scavenging of OH^\cdot by H_2 can then create an additional H^\cdot . These radicals can then suppress corrosion and scavenge radiolytic oxidants.
- (ii) Similar inhibition and scavenging processes are possible when only α -radiation is present. In this case the dissociation of water could be caused by the need to neutralize the oxygen vacancy caused by the ejection of an O atom from the surface caused by an α -recoil event.
- (iii) In the absence of any radiation fields, experiments on SIMFUELS show that H_2 activation can occur rapidly on epsilon particles. Since these particles are galvanically-coupled to the rare earth-doped (and, hence, conducting) UO_2 matrix, they act as anodes forcing the matrix to adopt a low potential. For either a sufficiently high extent of simulated burn-up (number density of particles) at low $[H_2]$ or a sufficiently high $[H_2]$ at a low extent of simulated burn-up, this galvanic coupling can render the UO_2 unreactive.
- (iv) It is also possible that the UO_2 could activate H_2 in the presence of H_2O_2 , although evidence for this is weak. If oxidation/corrosion of the surface by H_2O_2 involves OH^\cdot , these could be scavenged by reaction with H_2 and hence prevented from causing fuel oxidation.

The studies show that even small pressures of H_2 (0.1 to 1 bar) can effectively suppress fuel corrosion. Since the production of H_2 will commence as soon as waste containers fail and groundwater contacts the carbon steel liner, and, in sealed repositories, H_2 pressures up to 50 bar are anticipated, this influence of H_2 has the potential to shut down fuel corrosion very rapidly. This suppression will be at least partially effective even for early failure when oxidizing conditions would be maintained by gamma/beta radiolysis of water. It is possible therefore that the conditions for extremely slow chemical dissolution of fuel would be rapidly established and that dissolution and radionuclide release would be extremely slow almost from the time of container failure irrespective of when it occurred.

5. ACKNOWLEDGEMENTS

This research was funded under the Industrial Research Chair agreement between the Natural Sciences and Engineering Research Council (NSERC, Ottawa) and the Nuclear Waste management Organization (NWMO, Toronto). The author would like to thank Kastriot Spahiu (Swedish Nuclear Fuel and Waste Management Company, Stockholm, Sweden) for extensive discussions, suggested interpretations of available data, and guidance in the location of key references.

REFERENCES

- Ai, M. 1983. The reaction of formaldehyde on various oxide catalysts. *J. Catal.* 83, 141.
- Albinsson, Y., A. Odegaard- Jensen, V.M. Oversby and L.O. Werme. 2003. Leaching of spent fuel under anaerobic and reducing conditions. *Mat. Res. Soc. Symp. Proc.* Vol. 757, 407-413.
- Bailey, M.G., L.H. Johnson and D.W. Shoesmith. 1985. Effects of alpha radiolysis of water on the corrosion of UO_2 . *Corros. Sci.* 25, 233-238.
- Blackwood, D.J., C.C. Naish, N. Platts, K.J. Taylor and M.I. Thomas. 1995. The anaerobic corrosion of carbon steel in granite groundwater. Swedish Nuclear Fuel and Waste Management Company Technical Report TR-95-03.
- Broczkowski, M.E., J.J. Noël and D.W. Shoesmith. 2005. The inhibiting effects of hydrogen on the corrosion of uranium dioxide under nuclear waste disposal conditions. *J. Nucl. Mater.* 346, 16-23.
- Broczkowski, M.E., J.J. Noël and D.W. Shoesmith. 2007. The influence of dissolved hydrogen on the surface composition of doped uranium dioxide under aqueous corrosion conditions. *J. Electroanal. Chem.* 602, 8-16.
- Broczkowski, M.E., R. Zhu, Z. Ding, J.J. Noël and D.W. Shoesmith. 2006. Electrochemical, SECM and XPS studies of the influence of H_2 on UO_2 nuclear fuel corrosion. *Mat. Res. Soc. Symp. Proc.* Vol. 932, 449-456.
- Broczkowski, M.E. 2008. The effects of hydrogen and temperature on the electrochemistry and corrosion of uranium dioxide. Ph.D. Thesis. The University of Western Ontario, London, Ontario.
- Carbol, P., J. Cobos-Sabate, J-P. Glatz, C. Ronchi, V. Rondinella, D.H. Wegen, T. Wiss, A. Loida, V. Metz, B. Kienzler, K. Spahiu, B. Grambow, J. Quinones, A. Martinez Esparza Valiente. 2005. The effect of dissolved hydrogen on the dissolution of ^{233}U -doped UO_2 (s), high burn-up spent fuel and MOX fuel. Swedish Nuclear Fuel and Waste Management Company Technical Report TR-05-09.
- Clarens, F., J. de Pablo, I. Diaz-Perez, I. Casas, J. Gimenez and M. Rovira. 2004. Formation of studtite during the oxidative dissolution of UO_2 by hydrogen peroxide. *Environ. Sci. Technol.* 38, 6656-6661.

- Corbel, C., G. Sattonnay, S. Guilbert, F. Garrido, M-F. Barthe and C. Jegou. 2006. Addition versus radiolytic production effects on aqueous corrosion of UO_2 . *J. Nucl. Mater.* 348, 1-17.
- Cui, D. and T. Eriksen. 1996. Reduction of Tc(VII) and Np(V) in solution by ferrous ion. A laboratory study of homogeneous and heterogeneous redox processes. Swedish Nuclear Fuel and Waste Management Company Report SKB TR-96-03.
- Cui, D., K. Spahiu and P. Wersin. 2003. Redox reactions of iron and uranium dioxide in simulated cement pore water under anoxic conditions. *Mat. Res. Soc. Symp. Proc.* 757, 427-432.
- Cui, D., J. Low, C.J. Sjostedt, K. Spahiu. 2004. On Mo-Ru-Tc-Pd-Rh alloy particles extracted from spent fuel and their leaching behaviour under repository conditions. *Radiochim. Acta.* 92, 551-555.
- de Pablo, J., I. Casas, F. Clarens, F. El Aamrani and M. Rovira. 2001. The effect of hydrogen peroxide concentration on the oxidative dissolution of unirradiated uranium dioxide. *Mat. Res. Soc. Symp. Proc.* Vol. 663, 409-426.
- de Pablo, J., I. Casas, J. Gimenez, F. Clarens, L. Duro and J. Bruno. 2004. The oxidative dissolution mechanism of uranium dioxide. The effect of pH and oxygen partial pressure. *Mat. Res. Soc. Symp. Proc.* Vol. 807, 1-6.
- de Pablo, J., I. Casas, J. Gimenez, V. Marti and M.E. Torrero. 1996. Solid surface evolution model to predict uranium release from unirradiated UO_2 and nuclear spent fuel dissolution under oxidizing conditions. *J. Nucl. Mater.* 232, 138-145.
- Devoy, J., J. Haschke, D. Cui, K. Spahiu. 2003. Behaviour of spent fuel: chemistry and catalysis in the UO_2 -water system. *Mat. Res. Soc. Symp. Proc.* Vol. 807, 41-46.
- Ekeroth, E. and M. Jonsson. 2003. Oxidation of UO_2 by radiolytic oxidants. *J. Nucl. Mater.* 242-248.
- Ekeroth, E., M. Jonsson, T.E. Eriksen, K. Ljungquist, S. Kovacs and J. Puigdomenech. 2004. Reduction of UO_2^{2+} by H_2 . *J. Nucl. Mater.* 334, 35.
- Ekeroth, E., O. Roth and M. Jonsson. 2006. The relative impact of radiolysis products in radiation induced oxidative dissolution of UO_2 . *J. Nucl. Mater.* 355, 38-46.
- El Aamrani, F., I. Casas, C. Martin, M. Rovira and J. de Pablo. 1998. Effect of iron and canister corrosion products on the dissolution of UO_2 . In: *Proceedings Spent Fuel Workshop 1998*. Las Vegas, Nevada.
- Eriksen, T. 1996. Radiolysis of water within a ruptured fuel element. Swedish Nuclear Fuel and Waste management Company Progress Report U-96-29.
- Fanghanel, Th. and V. Neck. 2002. Aquatic chemistry and solubility phenomena of actinide oxides/hydroxides, *Pure and Applied Chemistry.* 74, 1895-1907.

- Fuger, J. 1993. Problems in the thermodynamics of the actinides in relation with the back-end of the nuclear cycle. *J. Nucl. Mater.* 201, 3-14.
- Gimenez, J., E. Baraj, M. E. Torrero, I. Casas and J. de Pablo. 1996. Effect of H₂O₂, NaClO, and Fe on the dissolution of unirradiated UO₂ in NaCl 5 mol·kg⁻¹. Comparison with spent fuel dissolution experiments. *J. Nucl. Mater.* 238, 64-69.
- Goldik, J.S., J.J. Noël and D.W. Shoesmith. 2005. The electrochemical reduction of hydrogen peroxide on uranium dioxide electrodes in alkaline solution. *J. Electroanal. Chem.* 582, 241-248.
- Goldik, J.S., J.J. Noël and D.W. Shoesmith. 2006. The effects of simulated fission products in the reduction of hydrogen peroxide on simulated nuclear fuel electrodes. *J. Electrochem. Soc.* 153, E151-E159.
- Grambow, B., R.S. Forsyth, L.O. Werme and J. Bruno. 1990. Fission product release from spent UO₂ fuel under uranium saturated oxic conditions. *Nuclear Technology.* 92, 202-213.
- Grambow, B., A. Loida, P. Dressler, H. Geckeis, J. Gago, I. Casas, J. de Pablo, J. Gimenez, M.E. Torrero. 1996. Long-term safety of radioactive waste disposal: Chemical reaction of fabricated and high burn-up spent fuel with saline brines, Forschungszentrum Karlsruhe, Wissenschaftliche Berichte FZKA 5702.
- Grambow, B., A. Loida, A. Martinez-Esparza, P. Diaz-Arocas, J. de Pablo, G. Marx, J.P. Glatz, K. Lemmens, K. Ollila and H. Christensen. 2000. Source term for performance assessment of spent fuel as a waste form. European Commission, Nuclear Science and Technology Report EUR 19140 EN.
- Grambow, B., E. Smailos, H. Geckeis, R. Muller and H. Hentschel. 1996. Sorption and reduction of uranium (VI) on iron corrosion products under reducing saline conditions, *Radiochim. Acta.* 74, 149-154.
- Grambow, B., T. Mennecart, M. Fattahi, and G. Blondinaux. 2004. Electrochemical aspects of radiolytically enhanced UO₂ dissolution, *Radiochim. Acta.* 92, 603-609.
- Grasselli, R.K., J.D. Burrington, D.D. Suresh, M.S. Friedrich and M.A.S. Hazle. 1981. Ammoxidation of α -methylstyrene to acrylonitrile over a U-Sb-oxide catalysts. *J. Catal.* 68, 109.
- Graselli, R.K. and D.D. Suresh. 1972. Aspects of structure and activity in U...Sb oxide acrylonitrile catalysts. *J. Catal.* 25, 273-291.
- Grenthe, I., J. Fuger, R.J. Konings, R.J. Lemire, A.B. Muller, C. Nguyen-Trung and H. Wanner. 1992. Chemical thermodynamics of uranium. North Holland, Amsterdam.
- Guillamont, R., T. Fanghanel, I. Grenthe, V. Neck, D. Palmer, and M.H. Rand. 2003. Update on the chemical thermodynamics of uranium, neptunium, plutonium, americium and

- technetium, OECD-NEA. Chemical Thermodynamics. 5, 182-187, Elsevier, Amsterdam, Netherlands.
- Guppy, R.M., A. Atkinson and T.M. Valentine. 1989. Studies of the solubility of technetium under a range of redox conditions. Harwell ARE-R 13467, DOE/RW/89/102.
- Hansen, H.C.B. 2002. Environmental chemistry of iron (II) – iron (III) LDHs (green rusts). Chapter 13 in Rives, V. (editor). Layered double hydroxides: Present and Future. 413-434. Nova Sci. Publ. New York, New York.
- Haschke J.M., T.H. Allen and J.L. Stakebake. 1996. Reaction kinetics of plutonium with oxygen, water and humid air. J. Allys and Compounds. 243, 23-35.
- Heneghan, C.S., G.J. Hutchings, S.R. O'Leary, S.H. Taylor, V.J. Boyd and I.D. Hudson. 1999. A temporal analysis of products study of the mechanism of VOC catalytic oxidation using uranium oxide catalysts. Catal Today. 54.
- Hossain, M.M., E. Ekeröth and M. Jonsson. 2006. Effects of HCO_3^- on the kinetics of UO_2 oxidation by H_2O_2 . J. Nucl. Mater. 358, 202-208.
- Jegou, C., V. Broudie, A. Poulesquen and J.M. Bart. 2004. Effects of α and γ - radiolysis of water on alteration of the spent fuel UO_2 nuclear fuel matrix. Mat. Res. Soc. Symp. Proc. Vol. 807, 391-396.
- Johnson, L.H. and D.W. Shoemith. 1988. Spent Fuel. In radioactive waste forms for the future (W.B. Lutze and R.C. Ewing, editors). Elsevier Science Publishers. Amsterdam, Netherlands.
- Jonsson, M., F. Nielsen, E. Ekeröth and T. Eriksen. 2003. Modelling of the effects of radiolysis on UO_2 dissolution employing recent experimental data. Mat. Res. Soc. Symp. Proc. Vol. 807, 385-390.
- Jonsson, M., F. Nielsen, O. Roth, E. Ekeröth, S. Nilsson and M.M Hossain. 2007. Radiation induced spent nuclear fuel dissolution under deep repository conditions, Environ. Sci. Technol. 41, 7087-7093.
- King, F. and D.W. Shoemith. 2004. Electrochemical studies of the effect of H_2 on UO_2 dissolution, Swedish Nuclear Fuel and Waste Management Company Technical Report TR-04-20.
- King, F. and M. Kolar. 1996. Modeling the consumption of oxygen by container corrosion and reaction with Fe (II). Mat. Res. Soc. Symp. Proc. Vol. 412, 547-554.
- King, F. and M. Kolar. 2000. The copper container corrosion model used in AECL'S second case study. Ontario Power Generation Report 06819-REP-01200-10041-R00.
- King, F. and M. Kolar. 2002b. Sensitivity analysis of the factors affecting the effective G-value, G_{EFF} , in the mixed potential model for used fuel dissolution. Ontario Power Generation Report 06819-REP-01300-10044-R00.

- King, F. and M.Kolar. 2002a. Validation of the mixed-potential model for used fuel dissolution against experimental data. Ontario Power Generation Report 06819-REP-01200-10077-R00.
- King, F., M.J. Quinn and N.H. Miller. 1999. The effect of hydrogen and gamma radiation on the oxidation of UO_2 in $0.1 \text{ mol}\cdot\text{L}^{-1}$ NaCl, solution. Swedish Nuclear Fuel and Waste Management Company Report TR-99-27.
- King, F. and S. Stroes-Gascoyne. 2000. An assessment of the long-term corrosion behaviour of C-steel and the impact on the redox conditions inside a nuclear fuel waste disposal container. Ontario Power Generation Report 06819-REP-01200-10028-R00.
- Kleykamp, H. 1985. The chemical state of the fission products in oxide fuels. *J. Nucl. Mater.* 131, 221-246.
- Kleykamp, H. 1988. The chemical state of fission products in oxide fuels at different stages of the nuclear fuel cycle. *Nuclear technology.* 80, 412-422.
- Lee, C.T., Z. Qin, M. Odziemkowski and D.W. Shoesmith. 2005. The influence of groundwater anions on the impedance behavior of carbon steel corroding under anoxic conditions. *Electrochim. Acta.* 51, 1558-1568
- Liu, L. and I. Neretnieks. 1995. Some evidence of radiolysis in a uranium ore body – quantification and interpretation. *Mat. Res. Soc. Symp. Proc.* Vol. 353, 1179-1186.
- Liu, L. and I. Neretnieks. 2002. The effect of hydrogen on the oxidative dissolution of spent fuel. *Nuclear Technology.* 138, 69-77.
- Loida, A., B. Grambow and H. Geckeis. 1996. Anoxic corrosion of various high burn-up spent fuel samples. *J. Nucl. Mater.* 238, 11-22.
- Loida, A., B. Grambow and H. Geckeis. 2001. Congruent and incongruent radionuclide release during matrix dissolution of partly oxidized high burn-up spent fuel. *Mat. Res. Soc. Symp. Proc.* 663, 417-426.
- Loida, A., B. Kienzler and H. Geikis. 2002. Mobilization/retention of radionuclides during co-dissolution of high burn-up spent fuel and near field materials in salt brines. *Mat. Res. Soc. Symp. Proc.* Vol. 757, 433-439
- Loida, A., M. Kelm, B. Kienzer, H. Geckeis and A. Bauer. 2006. The effect of near field constraints on the corrosion behavior of high burn-up spent fuel. *Mat. Res. Soc. Symp. Proc.* Vol. 932, 473-480.
- Lucuta, P.G., R.A. Verrall, H.J. Matzke and B.J.F. Palmer. 1991. Microstructural features of SIMFUEL-simulated high burn-up UO_2 -based nuclear fuel. *J. Nucl. Mater.* 178, 48-60.
- Maak, P. 2003. Development of a used fuel container for nuclear fuel waste. *Mat. Res. Soc. Symp. Proc.* Vol. 807, 447.

- Madhavaram, H. and H. Idriss. 1999. Evidence of furan formation from ethanol over β - UO_3 . *J. Catal.* 184, 553
- Madhavaram, H. and H. Idriss. 2002. Carbon efficiency and the surface chemistry of the actinides: direct formation of furan from acetylene over β - UO_3 . *J. Catal.* 206, 155.
- McMurry, J., D.A. Dixon, J.D. Garroni, B.M. Ikeda, S. Stroes-Gascoyne, P. Baumgartner and T.W. Melnyk. 2003. Evolution of a Canadian deep geologic repository: base scenario. Ontario Power Generation Report 06819-REP-01200-10092-R00.
- Mennecart, T., B. Grambow, M. Fattahi, G. Blondiaux and Z. Andriambololona. 2004. Effect of alpha radiolysis on UO_2 dissolution under reducing conditions. *Mat. Res. Soc. Symp. Proc.* Vol. 807, 403-408.
- Neck, V. and J.I. Kim. 2001. Solubility and hydrolysis of tetravalent actinides. *Radiochim. Acta.* 89, 1-16.
- Neck, V., M. Altmaier, R. Muller, M. Schlieker, and T. Fanghanel. 2003. Solubility of U(VI) in NaCl and MgCl_2 solutions. Ninth International Conference on Chemistry and Migration Behaviour of Actinides and Fission Products in the Geosphere, Migration '03, 47.
- Nielsen, F. and M. Jonsson. 2006. Geometrical α - and β - dose rate distributions and production rates of radiolysis products in water in contact with spent nuclear fuel. *J. Nucl. Mater.* 359, 1-7.
- Nilsson, S. and M. Jonsson. 2007. On the catalytic effects of $\text{UO}_2(\text{s})$ and $\text{Pd}(\text{s})$ on the reaction between H_2O_2 and H_2 in aqueous solution. *J. Nucl. Mater.* 372, 160-163
- Nilsson, S. and M. Jonsson. 2008. On the catalytic effect of $\text{Pd}(\text{s})$ on the reduction of UO_2^{2+} with H_2 in aqueous solution. *J. Nucl. Mater.* 374, 290-292.
- Nilsson, S. 2008. Influence of metallic fission products and self irradiation on the rate of spent nuclear fuel-matrix dissolution. Licentiate Thesis in Chemistry. Royal Institute of Technology. Stockholm. Paper V.
- Norskov, J.K., T. Bligaard, A. Lagodottir, J.R. Kitchin, J.G. Chen, S. Pandelov and U. Stimming. 2005. Trends in exchange currents for hydrogen evolution. *J. Electrochem. Soc.* 152, J23-J26.
- Nuclear Waste Management Organization (NWMO). 2005. Choosing a way forward: The future management of Canada's used nuclear fuel. (Available at: www.nwmo.ca)
- Ollila, K., Y. Albinsson, V. Oversby and M. Cowper. 2003. Dissolution rates of unirradiated UO_2 , UO_2 doped with ^{233}U and spent fuel under normal atmospheric conditions and under reducing conditions using an isotope dilution method. Swedish Nuclear Fuel and Waste Management Company Technical Report TR-03-13.
- Parks, G.A. and D.C. Pohl. 1988. Hydrothermal solubility of uraninite. *Geochim. Cosmochim. Acta.* 52, 863-875.

- Pastina, B., J. Isabey and B. Hickel. 1999. The influence of water chemistry on the radiolysis of primary coolant water in pressurized water reactors. *J. Nucl. Mater.* 264, 309-318.
- Pastina, B. and J.A. Laverne. 2001. Effect of molecular hydrogen on hydrogen peroxide in water radiolysis. *J. Phys. Chem. A.* 105, 9316-9322.
- Petrik, N.G., A.B. Alexandrov and A.I. Vall. 2001. Interfacial energy transfer during gamma radiolysis of water on the surface of ZrO_2 and some other oxides. *J. Phys. Chem. B.* 105, 5935-5944.
- Poinssot, C., C. Ferry, M. Kelm, B. Grambow, A. Martinez-Esparza, L. Johnson, Z. Andriambololona, J. Bruno, C. Cachoir, J-M. Cavendon, H. Christensen, C. Corbel, C. Jegou, K. Lemmens, A. Loida, P. Lovera, F. Miserque, J. de Pablo, A. Poulesquen, J. Quinones, V. Rondinella, K. Spahiu and D. Wegen. 2005. Final report of the European project spent fuel stability under repository conditions. European Commission Report CEA-R-6093.
- Quinones, J., J.A. Serrano, P. Diaz-Arocas, J.L. Rodriguez-Almazan, J. Cobos, J.A. Esteban and A. Martinez-Esparza. 2001. Influence of container base material (Fe) on SIMFUEL leaching behaviour. *Mat. Res. Soc. Symp. Proc.* Vol. 663, 435-439.
- Rai, D., A.R. Felmy and J.L. Ryan. 1990. Uranium (IV) hydrolysis constants and solubility product of $UO_2 \cdot xH_2O$ (am). *Inorg. Chem.* 29, 260-264.
- Rai, D., M. Yui and D.A. Moore. 2003. Solubility and solubility product at 22°C of UO_2 precipitated from aqueous U(IV) solutions. *J. Solution Chem.* 32, 1-17.
- Rollin, S., K. Spahiu and U.B. Eklund. 2001. Determination of dissolution rates of spent fuel in carbonate solutions under different redox conditions with a flow-through experiment. *J. Nucl. Mater.* 297-231.
- Santos, B.G., H.W. Nesbitt, J.J. Noël and D.W. Shoesmith. 2004. X-ray photoelectron spectroscopy study of anodically oxidized SIMFUEL surfaces. *Electrochim. Acta.* 49, 1863-1873.
- Sellin, P. 2001. Hydromechanical evolution in a defective canister. *Mat. Res. Soc. Symp. Proc.* Vol. 663, 755-763.
- Senanayake, S.D., G.I.N. Waterhouse, A.S.Y. Chan, T.E. Madey, D.R. Mullins and H. Idriss. 2007. The reactions of water vapour on the surfaces of stoichiometric and reduced uranium dioxide: a high resolution XPS study. *Catal. Today.* 120, 151-157.
- Shoesmith, D.W. 2000. Fuel corrosion processes under waste disposal conditions. *J. Nucl. Mater.* 282, 1-31.
- Shoesmith, D.W. 2007. Used Fuel and Uranium Dioxide Dissolution Studies – A Review. Nuclear Waste Management Report, NWMO-TR-2007-03.
- Shoesmith, D.W., S. Sunder, M.G. Bailey and G.J. Wallace. 1989. Corrosion of nuclear fuel in oxygenated solutions. *Corros. Sci.* 29, 1115-1128.

- Shoesmith, D.W. and S. Sunder. 1991. An electrochemistry-based model for the dissolution of UO_2 . Atomic Energy of Canada Report, AECL-10488.
- Shoesmith, D.W., J.J. Noël, and F. Garisto. 2004. An experimental basis for a mixed potential model for nuclear fuel corrosion within a failed nuclear waste container. *Mat. Res. Soc. Symp. Proc.* Vol. 824, 81-88.
- Shoesmith, D.W., M. Kolar and F. King. 2003. A mixed potential model to predict fuel (uranium dioxide) corrosion within a failed nuclear waste container. *Corrosion.* 59, 802-816.
- Shoesmith, D.W., S. Sunder and W.H. Hocking. 1994. Electrochemistry of UO_2 nuclear fuel, in *Electrochemistry of Novel Materials* (edited by J. Lipkowski and P.N. Ross). VCH Publishers. New York, Chapter 6, 297-337.
- Smart, N.R., D.J. Blackwood, and L. Werme. 2002a. Anaerobic corrosion of carbon steel and cast Iron in artificial groundwater. Part I- Electrochemical aspects. *Corrosion.* 58, 547-559.
- Smart, N.R., D.J. Blackwood and L. Werme. 2002b. Anaerobic corrosion of carbon steel and cast iron in artificial groundwater. Part II – Gas generation. *Corrosion.* 58, 627-637.
- Spahiu, K., U-B. Eklund, D.Cui and M.Lundstrom. 2002. The influence of near field redox conditions on spent fuel leaching. *Mat. Res. Soc. Symp. Proc.* Vol. 713, 633-638.
- Spahiu, K., J. Devoy, D. Cui and D. Lundstrom. 2004. The reduction of U(VI) by near field hydrogen in the presence of $\text{UO}_2(\text{s})$. *Radiochim. Acta.* 92, 597-603.
- Spahiu, K., D. Cui and M. Lundstrom. 2004. The fate of radiolytic oxidants during spent fuel leaching in the presence of dissolved near field hydrogen. *Radiochim. Acta.* 92, 625-629.
- Stroes-Gascoyne, S., F.King, J.S. Betteridge. 2002a. The effects of alpha-radiolysis on UO_2 dissolution determined from electrochemical experiments with ^{238}Pu -doped UO_2 . Ontario Power Generation Report 06819-REP-01300-10030-R00
- Stroes-Gascoyne, S., F. King, J.S. Betteridge and F. Garisto. 2002b. The effects of alpha-radiolysis on UO_2 dissolution determined from electrochemical experiments with ^{238}Pu -doped UO_2 . *Radiochim. Acta.* 90, 603-609
- Stroes-Gascoyne, S. and J.S. Betteridge. 2005. The effects of doping level, carbonate, Fe and H_2 on the corrosion potential and dissolution rate of ^{238}Pu -doped UO_2 . In: *Proceedings of the Canadian Nuclear Society Meeting on Waste Management, Decommissioning and Environmental Restoration for Canada's Nuclear Activities: current practices and future needs.* Ottawa, Ontario. May 8-11 (2005).
- Stumm, W. (editor). 1990. *Aquatic chemical kinetics. Reaction rates of processes in natural waters.* John Wiley. New York, New York.

- Sunder, S., D.W. Shoesmith, H. Christensen and N.H. Miller. 1992. Oxidation of UO_2 fuel by the products of gamma radiolysis of water. *J. Nucl. Mater.* 190, 78-86.
- Sunder, S., D.W. Shoesmith, M. Kolar and D.M. Leneveu. 1997. Calculation of used nuclear fuel dissolution rates under anticipated Canadian waste vault conditions. *J. Nucl. Mater.* 250, 118-130.
- Sunder, S., G.D. Boyer and N.H. Miller. 1990. XPS studies of UO_2 oxidation by alpha radiolysis of water at 100°C . *J. Nucl. Mater.* 175, 163-169.
- Sunder, S., N.H. Miller and D.W. Shoesmith. 2004. Corrosion of uranium dioxide in hydrogen peroxide solutions. *Corros. Sci.* 46, 1095-1111.
- Tait, J.C. and L.H. Johnson. 1986. Computer modeling of alpha radiolysis of aqueous solutions in contact with used UO_2 fuel. *Proceedings 2nd International Conference on Radioactive Waste Management*. Winnipeg, Manitoba, September 7-11, 1986. Canadian Nuclear Society. Toronto, Ontario. 611-615.
- Taylor, S.H., C.S. Heneghan, G.J. Hutchings and I.D. Hudson. 2000. The activity and mechanism of uranium oxide catalysts for the oxidative destruction of volatile organic compounds. *Catal. Today.* 59, 249-259.
- Torrero, M.E., E. Baraj, J. de Pablo, J. Gimenez and I. Casas. 1997. Kinetics of corrosion and dissolution of uranium dioxide as a function of pH. *J. Chem. Kinetics.* 29, 261-267.
- Werme, L., L.H. Johnson, V.M. Oversby, F. King, K. Spahiu, B. Grambow and D.W. Shoesmith. 2004. Spent fuel performance under repository conditions: a model for use in SR-Can. Swedish Nuclear Fuel and Waste Management Company, Technical Report TR-04-19.
- Wren, J.C., D.W. Shoesmith and S. Sunder. 2005. Corrosion behavior of uranium dioxide in alpha radiolytically decomposed water. *J. Electrochem. Soc.* 152, B470-B481.
- Yajima, T., Y. Kawamura and S. Ueta. 1995. Uranium (IV) solubility and hydrolysis constants under reducing conditions. *Mat. Res. Soc. Symp. Proc.* Vol. 353, 1137-1142.